Revised submission to Marine and Petroleum Geology
(Bight Basin Virtual Special Issue)

A second type of highly asphaltic crude oil seepage stranded on the South Australian coastline

Alexander J. Corrick*[1], Philip A. Hall[1], Se Gong[2], David M. McKirdy[1], David Selby[3, 4], Christine Trefry[5] and Andrew S. Ross[5]

[1] Department of Earth Sciences, School of Physical Sciences, University of Adelaide, SA 5005, Australia

[2] Energy, CSIRO, North Ryde, NSW 2113, Australia

[3] Department of Earth Sciences, Durham University, Durham DH1 3LE, UK

[4] State Key Laboratory of Geological Processes and Mineral Resources, School of Earth Resources, China University of Geosciences, Wuhan, 430074 Hubei, China

[5] Energy, CSIRO, Kensington, WA 6151, Australia

*** Corresponding author** (email: *alexander.corrick@adelaide.edu.au*)

HIGHLIGHTS (3-5 bullets, 85-character limit including spaces)

1) Report a new type of oil found on South Australian coastline termed asphaltic tar

2) Asphaltic tars share several source characteristics with well-studied asphaltites

3) Clear correlation to asphaltites is complicated by differences in thermal maturity

4) Asphaltic tars may have been altered by thermochemical sulphate reduction

ABSTRACT (296/300 words)

Strandings of semi-solid to solid asphaltic bitumen along the coastline of South Australia have been reported as far back as the late 1800s. Hitherto only a single variety, now referred to as asphaltite, has been attributed to seepage from the nearby Bight Basin. The geochemistry of the asphaltites suggest they were derived from a marine source rock deposited under anoxic or euxinic conditions, most likely a Cretaceous ocean anoxic event, and were generated within the early/main oil window. Here we identify a new type of semi-solid asphaltic bitumen collected following a severe storm event in 2016. Termed asphaltic tars, these viscous oils bear a strong geochemical resemblance to the asphaltites. Both oil types have high asphaltene contents, identical *n*-alkane carbon isotopic profiles and near identical source-specific sterane distributions. However, several notable geochemical variations can distinguish these new strandings from the asphaltites. The most notable of these differences include heavier bulk sulphur isotopic composition, extremely high abundances of Re and Os with distinct $^{187}Re/^{188}Os$ and $^{187}Os/^{188}Os$ values and thermal maturity parameters consistent with generation in the late oil window. The differences in sulphur isotopic composition and Re-Os systematics could be considered evidence that despite their other source-specific similarities, the asphaltic tars originated from a different source rock. However, alteration of these two parameters can occur due to thermochemical sulphate reduction. Conclusive identification of this alteration process typically relies on further diagnostic parameters which are unfortunately not available in the case of coastal oil strandings. This introduces uncertainty to the correlation of these two types of asphaltic oil. In either scenario, the similarities between these two types of oil suggest their source rock(s) contained highly comparable organic matter inputs. We therefore attribute the origin of these new asphaltic tar strandings to natural seepage from the offshore Bight Basin.

KEYWORDS (maximum of 8)

- Bight Basin; asphaltite; asphaltic tar; oil-oil correlation; CSIA; sulphur isotopes; Re-Os; thermochemical sulphate reduction

1. INTRODUCTION

Ocean beaches along Australia's southern margin are known to collect bitumen emitted from seafloor seeps associated with a variety of different petroleum systems (e.g. McKirdy et al., 1986, 1994; Padley, 1995; Edwards et al., 1998, 2016, 2018). Reports of asphaltene-rich coastal bitumen strandings (asphaltum, now referred to as asphaltite) in the region date back to the early 1800s and continue to the present (Trewartha, 1850; Tolmer, 1882; Sprigg and Woolley, 1963; Volkman et al., 1992; Edwards et al., 1998; Hall et al., 2014; Ross et al., 2017). Historical reports of these asphaltite strandings predate anthropogenic inputs of hydrocarbons to the region, suggesting that they are the product of natural offshore seepage. Although asphaltite is the least common variety of coastal bitumen recognised along the Australian coastline, it contributes the largest specimens, with individual pieces weighing up to 7 kg (Edwards et al., 1998, 2016).

Source and maturity-specific biomarkers indicate that these asphaltites are derived from a Mesozoic marine shale, deposited under sub-oxic to euxinic conditions, which expelled petroleum within the early oil window (Edwards et al., 1998; Hall et al., 2014; Scarlett et al., 2019). The source rock is presently thought to have been deposited during an oceanic anoxic event (OAE). However, interpretations vary from the Cenomanian-Turonian OAE2 (Totterdell et al., 2008; Boreham, 2009; Hall et al., 2014; Corrick et al., 2019), the Albian OAE1d (Boult et al., 2005; Hall et al., 2014), the Aptian OAE1a and Albian OAE1b events (Scarlett et al., 2019). Inspection of the GeoMark^{TM} global petroleum database suggests that the asphaltites are not products of any documented petroleum system (Summons et al., 2001). Unlike the majority of the tar balls found along the South Australian coastline (viz. 'waxy bitumens') which have been geochemically linked to Cenozoic petroleum systems in southeast Asia (Padley, 1995; Edwards et al., 2016, 2018), the asphaltites are currently thought to originate from an undiscovered petroleum system in the offshore Bight Basin (Fig. 1A) located on Australia's southern margin (Boreham et al., 2001; Totterdell et al., 2008; Hall et al., 2014). This interpretation is supported by analysis of organic-rich samples with similar geochemistry dredged from the basin (Totterdell et al., 2008; Boreham, 2009) and rhenium-osmium (Re-Os) geochronology of the asphaltites (Corrick et al., 2019), which

demonstrated their timing of generation is consistent with existing petroleum systems models for the basin (Struckmeyer et al., 2001; Totterdell et al., 2008). Previous studies have also proposed seepage from other nearby basins, such as the Otway Basin (Boult et al., 2005; Hall et al., 2014). However, recent modelling of the metaocean conditions of the Great Australian Bight suggests that offshore seepage from the Otway Basin is unlikely to migrate west, a requirement given the observed spatial distribution of asphaltite strandings along the coastline (Ross et al., 2017). Seepage from the Ceduna or Duntroon sub-basins of the Bight Basin, however, is consistent with the documented regions of asphaltite stranding (Ross et al., 2017).

The Bight Basin comprises an approximately 15 km-thick succession of Late Jurassic to Cretaceous sediments (Fig. S1) deposited in response to the separation of Australia and Antarctica during the break-up of the supercontinent Gondwana (Fraser and Tilbury, 1979; Totterdell et al., 2000; Totterdell and Bradshaw, 2004). These Mesozoic deposits are unconformably overlain by Palaeogene sediments with no source potential (Totterdell et al., 2008). Proposed petroleum systems in the basin are primarily associated with thick mid- to late Cretaceous deltaic and marine sediments, namely the Blue Whale, White Pointer, Tiger and Hammerhead supersequences (Blevin et al., 2000; Struckmeyer et al., 2001; Totterdell et al., 2000, 2008). However, no working petroleum systems have yet been proven within the basin.

Aside from the asphaltite strandings, no other seeped hydrocarbons that have been found on the South Australian coastline are considered products of the Bight Basin. In this study we report a new variety of asphaltene-rich crude oil stranded on the southeastern coastline of South Australia in October 2016. Referred to herein as asphaltic tar, these new strandings display strong geochemical similarities to the asphaltites, suggesting that the two oil types may originate from lateral equivalents of the same source rock.

2. MATERIALS AND METHODS

2.1. Sample suite

The stranding locations of the specimens analysed in this study are shown in Figure 1A and their collection details are summarised in Table S1. Details of the four representative waxy bitumen samples also included in this study to illustrate their contrasting *n*-alkane $\delta^{13}C$ profiles may be found in Ross et al. (2017). The asphaltites are visually distinctive, jet black, semi-solid to solid bitumens with a petroliferous odour and commonly exhibit deep shrinkage cracks (Fig. 1B). Fresh specimens with a soft and slightly pliable interior are rare, as most asphaltites collected on the coastline have become brittle, breaking apart with a diagnostic conchoidal fracture. The asphaltic tars are similarly jet black in colour but emit a stronger petroliferous odour and have remained viscous and sticky with a surficial sand coating (Fig. 1C).

The specimens compared in this study were recovered during three systematic annual surveys of 30 ocean beaches spanning the South Australian coastline in the period 2014 to 2016, as part of the Great Australian Bight Research Program (Ross et al., 2017). The sample suite was further supplemented with additional samples donated from private collections. Representative asphaltites were selected from each of the three surveys while ensuring a spatial distribution that encompassed the entire survey area (Fig. 1A). Asphaltic tar samples were only encountered in the final survey conducted in October of 2016, at the Number 1 and 2 Rocks beach in the Canunda National Park, located on the Bonney Coast approximately 40 km west of Mount Gambier. This survey occurred 24 days after a one-in-fifty-year storm event that affected much of the South Australian coastline (Bureau of Meteorology, 2016; Burns et al., 2017) and found the spatial distribution of coastal bitumen deviated significantly from the previous two surveys (Ross et al., 2017).

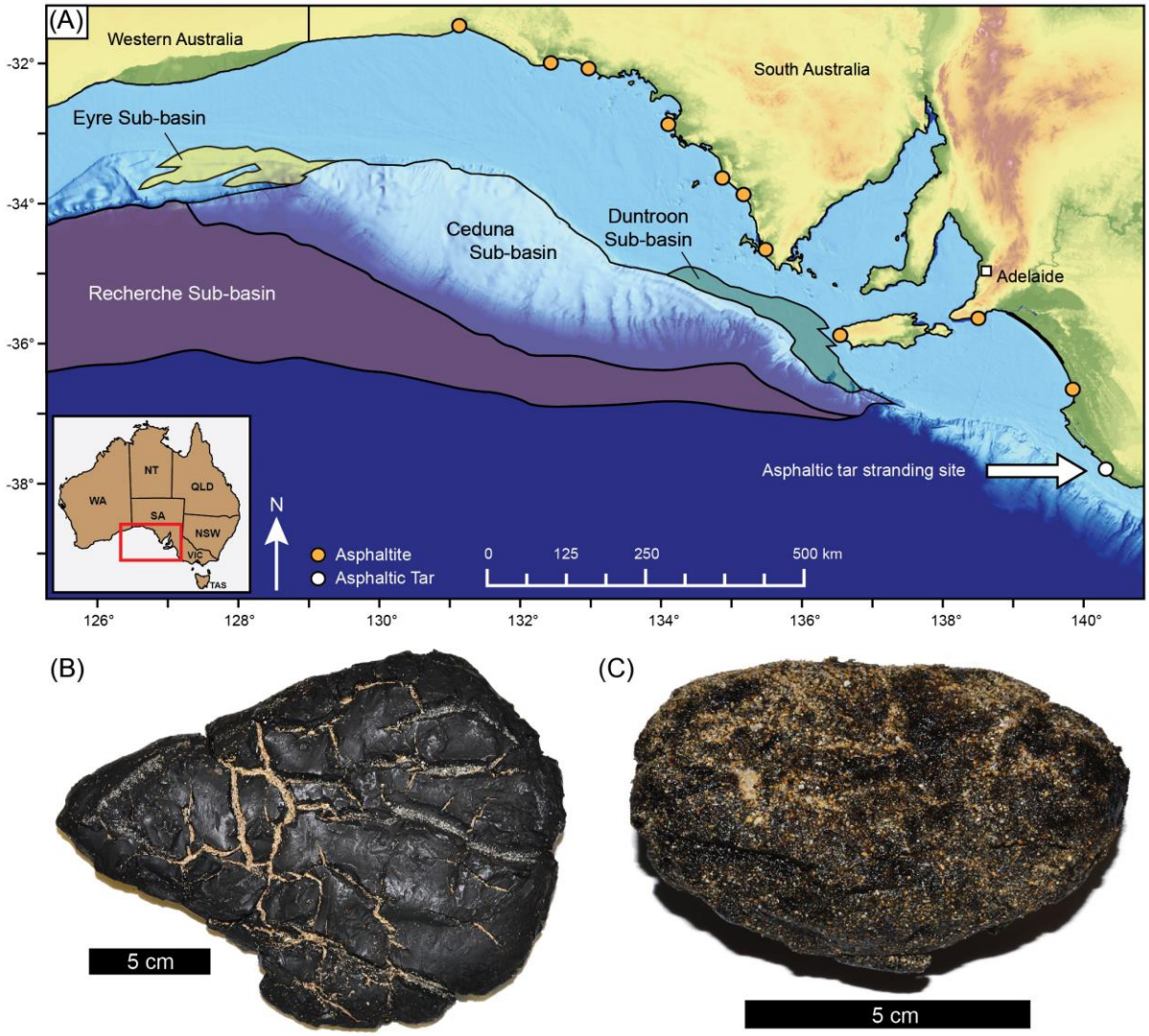

Figure 1: (A) Locations of analysed asphaltite and asphaltic tar samples and the Jurassic-Cretaceous sub-basins of the offshore Bight Basin. (B) Photograph of asphaltite sample W13/007507 collected from Waitpinga Beach in 2014, exhibiting characteristic shrinkage cracks. (C) Photograph of asphaltic tar sample /001059 collected from Number 1 and 2 Rocks in 2016.

2.2. Bulk bitumen analyses

2.2.1. Whole-oil gas chromatography-mass spectrometry

A sub-sample (≤200 mg) was removed from each bitumen specimen and dissolved in 10 mL of dichloromethane/methanol (93:7, v:v). An aliquot of this solution was used for whole-oil GC-MS. Analyses of the samples collected in 2014 and 2015 were performed on an Agilent 6890 gas chromatograph interfaced with a 5973N MSD (electron energy 70 eV) and tuned using automatic setup parameters for each sequence. Chromatography was carried out on an Agilent HP-5MS fused silica column (30 m x 0.25 mm i.d. x 0.25 µm film thickness), using either a split (50 mL/min) or splitless injection mode, the latter employed if split injection

data showed low responses. The oven was programmed at an initial temperature of 50°C for 1 min, followed by heating at 8°C/min to 300°C. The carrier gas was helium at a flow rate of 1 mL/min. GC-MS analyses of the samples collected in 2016 were performed on an Agilent 7890B gas chromatograph interfaced with a 5977B MSD (electron energy 70 eV) and tuned using automatic setup parameters for each sequence. Chromatography was carried out on a J&W DB-5MS fused silica column (30 m x 0.25 mm i.d. x 0.25 µm film thickness), using the same operating conditions as employed for the 2014 and 2015 samples. In both cases, whole-oil GC-MS was conducted in scan mode (scan interval 45–500 AMU at approx. 3 scans/sec).

2.2.2. Elemental analysis (EA)

The sulphur content (weight %) of each sample was determined using a Perkin Elmer 2400 series II CHNS/O Elemental Analyzer in CHNS configuration. The combined combustion/reduction tube was packed with Perkin Elmer EA6000 and Perkin Elmer 'Hi-Purity' Copper (reaction temperature of 975°C). Results were calibrated against a Perkin Elmer Organic Analytical Standard (cystine, 3–4 mg) with a known abundance of sulphur (26.69 ± 0.3%). The maximum uncertainty in sulphur content values was ±0.5%.

2.2.3. Elemental analysis – isotope ratio mass spectrometry (EA-IRMS)

Sulphur isotope data ($\delta^{34}S$) were collected using a Eurovector EuroEA Elemental Analyzer modified with a Valco valve to allow separation of combustion SO_2 from CO_2 and N_2. Results from interior subsamples of each bitumen specimen were calibrated to two in-house standards (S2 and S3) of silver sulphide (Ag_2S) with $\delta^{34}S$ values of +22.7‰ and -32.3‰, respectively. Due to the range in sulphur content between the asphaltites and asphaltic tars, results were calibrated against multiple weights of each standard (in the range 2–4 mg). The maximum uncertainty in $\delta^{34}S$ values was ±0.38‰.

2.2.4. Re-Os isotopic composition

Re-Os analysis of three asphaltic tars was conducted using the same analytical approach as that taken for the asphaltites by Corrick et al. (2019), based on the methods of Selby et al.

(2007). The precision for all Re-Os data was determined using full error propagation of all sources of uncertainty.

2.3. Analysis of saturated, aromatic and polar fractions

2.3.1. Oil fractionation

The saturated, aromatic and polar fractions were separated from 20 mg aliquots of whole bitumen using the procedure of Bastow et al. (2007). The recovered saturated hydrocarbons and polar fractions were stored in 2 mL chromatography vials, while the aromatics fraction was stored in 2 mL amber glass vials to ensure minimal degradation by ultraviolet light.

2.3.2. Separation of n-alkanes and branched/cyclic alkanes

Saturates fractions were dissolved in cyclohexane and transferred on to 5Å molecular sieve (activated at 450°C) before heating in an oven at 80°C overnight to ensure complete *n*-alkane absorption. The resulting branched/cyclic alkane fraction was used for biomarker analyses (see Sections 2.3.3 and 2.3.4). For selected samples, the separated *n*-alkanes were then retrieved for compound-specific isotope analysis by digesting the molecular sieve in approximately 8 mL of 40% hydrofluoric acid in a polytetrafluoroethylene test tube and extracting the released *n*-alkanes using *n*-pentane. The resulting *n*-alkane fractions were concentrated under a stream of nitrogen prior to further analysis.

2.3.3. Selected ion monitoring gas chromatography-mass spectrometry (SIM GC-MS)

GC-MS analysis of the branched/cyclic alkanes was performed on an Agilent 7890A gas chromatograph interfaced with a 5975C MSD (electron energy 70 eV) tuned using automatic setup parameters on the day of the analysis. Chromatography was carried out on a J&W DB-5MS fused silica column (60 m x 0.25 mm i.d. x 0.25 µm film thickness). A 1 µL aliquot of the branched/cyclic saturate fraction dissolved in petroleum ether was injected into the split/splitless injector at 300°C operating in split mode (20 mL/min). After being held at an initial temperature of 40°C for 2 min., the oven was heated at 20°C/min to 200°C and then ramped to 310°C at 2°C/min. The carrier gas was helium at a flow rate of 1.5 mL/min.

2.3.4. Gas chromatography tandem mass spectrometry (GC-MS-MS) with cold electron ionisation

GC-MS-MS analysis of the branched/cyclic alkanes was performed on a Perkin Elmer 680 Clarus gas chromatograph interfaced with a Perkin Elmer iQT Quadrupole Time of Flight (QToF) mass spectrometer fitted with a Cold-EI source and tuned using automatic setup parameters for each sequence. Chromatography was carried out on a J&W DB-5MS fused silica column (60 m x 0.25 mm i.d. x 0.25 µm film thickness). A 1 µL aliquot of saturates fraction dissolved in cyclohexane was injected at 300°C into the injector operating in splitless mode. The oven was held at an initial temperature of 50°C for 1 min., followed by heating at 12°C/min to 180°C and then at 4°C/min to 310°C. Helium was the carrier gas at a flow rate of 2 mL/min.

2.3.5. Carbon compound-specific isotope analysis (CSIA)

The carbon isotopic composition ($\delta^{13}C$) of individual *n*-alkanes from representative asphaltite, asphaltic tar and waxy bitumen samples was measured by gas chromatography-combustion-isotope ratio mass spectrometry using a 6890N GC connected to a GC-C/TC III combustion device coupled via open split to a Thermo MAT 253 mass spectrometer. The *n*-alkane fractions (1 µL) were injected into the inlet system in splitless mode (1 min). The injector was held at a temperature of 290°C. The *n*-alkanes were separated on a fused silica capillary column (SGE BP-5, 30 m x 0.25 mm ID, 0.25 mm film thickness). The GC oven was held at 50°C for 2 minutes, then heated at 25°C/min to 120°C, followed by a second heating ramp of 5°C/min to 310 °C, and finally held isothermal for 8 minutes. The analytes of the GC effluent stream were oxidised to CO_2 in the combustion furnace at 950°C on a CuO/NiO/Pt catalyst. The produced CO_2 was transferred on-line to the mass spectrometer to determine its $\delta^{13}C$ value. All results were calibrated to replicate measurements of individual *n*-alkanes from internal reference standards (IU A6 and B3). The maximum error in analytical precision was ±0.26‰.

2.3.6. GC-MS analyses of aromatic and polar fractions

Analyses of the aromatic and polar fractions were performed on a Perkin Elmer SQ8T/680 Clarus GC-MS fitted with a Perkin Elmer PE-5MS fused silica column (30 m x 0.25 mm i.d. x 0.25µm film thickness). A 1 µL aliquot was injected at 300°C into the injector operating in splitless mode. The oven was held at an initial temperature of 50°C for 1 min., followed by heating at 8°C/min to 300°C. Helium was the carrier gas at a flow rate of 1 ml/min. Data acquisition was conducted in scan mode (Scan 45:500AMU at approx. 3 scans/sec).

2.4. Asphaltene separation

The asphaltene content of each specimen was determined by dissolving a bulk sub-sample (0.3–0.7 g) in a minimum volume of dichloromethane/methanol (93:7). The asphaltene fraction was then precipitated by adding an excess of *n*-pentane. After the asphaltene precipitate settled from suspension, the maltene supernatant was removed using a Pasteur pipette and further *n*-pentane added. This process was repeated several times, until the maltene fraction had been entirely removed. The remaining asphaltene fraction was then rinsed with a final wash of *n*-pentane, dried and weighed.

3. RESULTS AND DISCUSSION

3.1. Comparison of source-specific saturated hydrocarbons

Source-specific biomarker parameters of the asphaltites and asphaltic tars are listed in Table 1. The freshest asphaltite specimen (W13/007976) preserves *n*-alkanes as light as C_8 (note that lighter gasoline-range *n*-alkanes would lie outside the detection range), with a slightly bimodal front-end distribution displaying maxima at C_{10} and C_{13}, thereafter decreasing in abundance towards C_{35} (Fig. 2A). Relative to this specimen, other asphaltites in the sample suite have less low-molecular-weight *n*-alkanes. This mild weathering results in a unimodal *n*-alkane distribution in the range C_{10}–C_{35}, with a maximum between C_{15} and C_{17} (Fig. 2B). Although the majority of samples selected for comparison were not significantly weathered asphaltites, two mildly degraded specimens (W13/007493 and W13/007668) are also included in the sample suite for reference. These samples contain less *n*-alkanes,

demonstrated by elevated Pr/C_{17} ratios compared to the other specimens. The asphaltic tar specimens preserve *n*-alkanes from C_9 to C_{35} with a maximum at C_{17} (Fig. 2C). Having been recovered from a single stranding location during one survey and being of highly uniform composition, the asphaltic tars are likely fragments of a single larger piece of tar separated by wave action during or shortly prior to stranding.

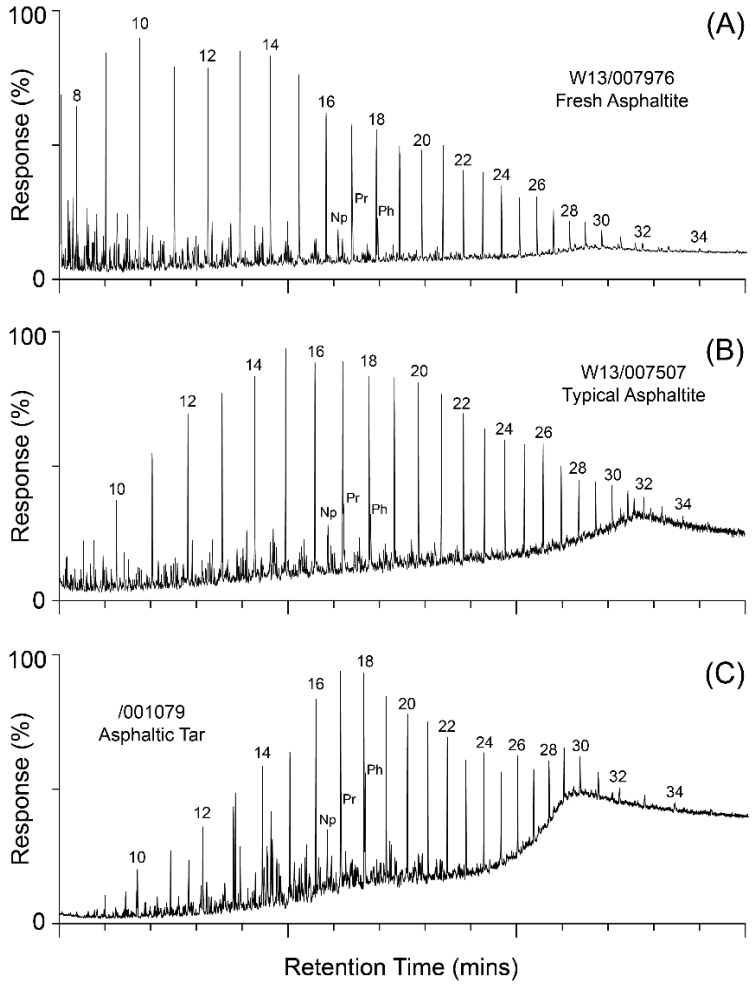

Figure 2: Whole-oil GC-MS total ion chromatograms for: (A) The freshest identified asphaltite specimen W13/007976; (B) A typical, lightly weathered asphaltite specimen W13/007507; and (C) An asphaltic tar specimen /001079; Np = norpristane, Pr = pristane, Ph = phytane, peak numbers correspond to *n*-alkane chain length.

The C_{27} : C_{28} : C_{29} and C_{27} Dia/(Dia+Reg) sterane ratios of both families are highly consistent (Fig. 3; Table 1). Some minor grouping of the two oils is based on the relative proportions of the C_{27} and C_{28} ααα 20*R* steranes. The asphaltic tars typically contain a slightly lower proportion of C_{27} steranes and slightly elevated C_{28} steranes. However, there remains some

overlap between the two oil types based on variability in these values in specific samples. The C_{31} (22R)/C_{30} αβ hopane ratios of the asphaltites and asphaltic tars are effectively identical, with respective values of 0.30–0.35 and 0.31–0.34, consistent with a marine source (Peters et al., 2005). This is supported in both oil families by the presence of diagnostic marine biomarkers such as dinosterane, a 4-methylsterane derived from marine dinoflagellates (Summons et al., 1987) and 24-*n*-propylcholestanes derived from marine chrysophyte algae (Moldowan et al., 1990). Furthermore, the complete lack of freshwater algal markers such as botryococcane (e.g. Moldowan and Seifert, 1980; McKirdy et al., 1986), and of angiosperm markers such as oleanane or bicadinanes (e.g. Edwards et al., 2018) together with a low abundance of tetracyclic polyprenoids (Holba et al., 2000) suggests negligible inputs from terrestrial or freshwater biota. Hence, the parent oils of both types of asphaltic bitumen originated from source rocks which contain only marine organic matter, consistent with the previously inferred source affinity of the asphaltites (Edwards et al., 1998; Hall et al., 2014).

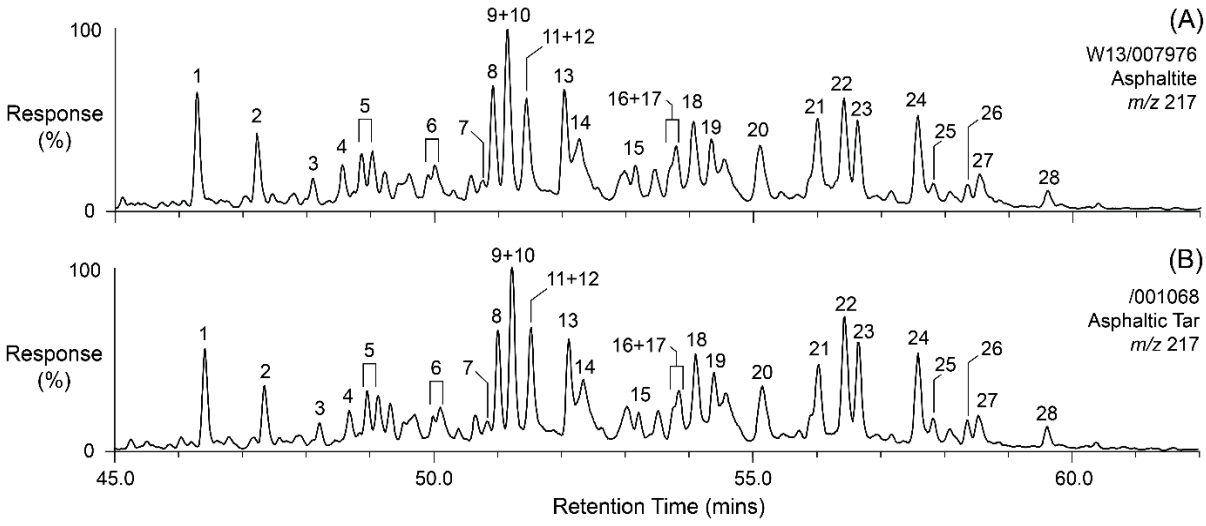

Figure 3: Partial *m/z* 217 chromatograms of representative asphaltite and asphaltic tar specimens demonstrating the similarity of their sterane and diasterane distributions. For a full list of peak assignments see Supplementary Information.

Table 1: Asphaltene content and selected biomarker parameters of asphaltite and asphaltic tar specimens. See Supplementary Information for explanation of compound abbreviations.

Samples	Asphaltene %	Sulphur %	$\delta^{34}S$ (‰)	Pr / Ph	Pr/C_{17}	27 : 28 : 29 ααα 20*R* steranes (*m/z* 217)	27 : 28 : 29 αββ (20*R*+*S*) steranes (*m/z* 218)	C_{27} Dia / (Dia+Reg) steranes (*m/z* 217)	C_{35} homohopane index (%)	C_{29} / C_{30} αβ hopane (*m/z* 191)	C_{31} (22*R*) / C_{30} αβ hopane (*m/z* 191)	C_{35} (22*S*) / C_{34} (22*S*) hopane (*m/z* 191)	Ts / (Ts+Tm)
Asphaltites													
W13/007472	59	4.0	-5.79	1.3	0.5	40 : 23 : 36	37 : 25 : 37	0.41	9.3	0.64	0.34	0.95	0.40
W13/007475	58	4.1	-6.58	1.3	0.5	38 : 23 : 39	38 : 26 : 37	0.45	7.8	0.65	0.33	0.90	0.41
W13/007476	53	4.3	-5.34	1.3	0.5	43 : 20 : 38	38 : 25 : 37	0.42	7.6	0.60	0.35	0.90	0.41
W13/007488	56	4.4	-5.30	1.2	0.5	43 : 20 : 37	38 : 25 : 37	0.43	8.6	0.64	0.33	0.92	0.39
W13/007493	52	4.1	-5.97	1.4	0.7	44 : 19 : 36	37 : 25 : 38	0.34*	8.3	0.69*	0.31	0.91	0.35
W13/007507	54	3.9	-5.66	1.2	0.5	40 : 27 : 33	39 : 25 : 36	0.43	7.4	0.65	0.32	0.79	0.40
W13/007516	55	4.0	-6.15	1.3	0.5	44 : 19 : 37	38 : 25 : 37	0.42	8.0	0.66	0.33	0.91	0.38
W13/007668	59	4.1	-7.18	1.1	1.3	37 : 27 : 36	37 : 26 : 37	0.45	7.7	0.67	0.30	0.90	0.38
W13/007671	54	3.8	-7.59	1.1	0.5	37 : 23 : 39	37 : 25 : 38	0.42	7.9	0.65	0.32	0.90	0.41
W13/007672	54	3.8	-7.34	1.2	0.4	43 : 20 : 37	39 : 25 : 36	0.43	8.4	0.65	0.33	0.94	0.38
W13/007845	51	3.7	-8.82	1.2	0.5	39 : 27 : 34	39 : 26 : 35	0.46	7.2	0.64	0.30	0.82	0.37
W13/007976	51	3.6	-7.80	1.2	0.4	38 : 26 : 36	38 : 25 : 37	0.45	7.6	0.62	0.30	0.82	0.41
Asphaltic Tars													
/001056	35	2.8	+2.61	0.7	0.6	35 : 29 : 36	36 : 26 : 38	0.43	11.0	0.82	0.32	1.02	0.22
/001063	22	3.2	+2.88	0.7	0.5	35 : 29 : 36	36 : 26 : 38	0.43	10.4	0.80	0.32	1.00	0.22
/001067	35	2.7	+4.84	0.7	0.6	34 : 29 : 37	35 : 25 : 40	0.43	11.3	0.78	0.33	1.03	0.22
/001068	25	3.2	+4.50	0.8	0.6	35 : 29 : 36	36 : 25 : 39	0.44	10.6	0.75	0.31	1.01	0.22
/001076	25	2.5	+4.27	0.7	0.5	37 : 26 : 37	36 : 23 : 42	0.43	11.0	0.79	0.34	1.05	0.27
/001079	27	3.0	+4.30	0.7	0.6	33 : 29 : 38	35 : 25 : 41	0.43	11.8	0.73	0.33	1.02	0.19
/001081	26	3.5	+4.85	0.7	0.5	32 : 29 : 38	35 : 25 : 40	0.44	11.8	0.76	0.33	1.04	0.19

* = Ratio variation attributed to significant weathering of the specimen

C_{27} Dia / (Dia + Reg) steranes = (C_{27} βα 20*S* + 20*R*) / [(C_{27} βα 20*S* + 20*R*) + (C_{27} ααα 20*S* + 20*R*)]

C_{35} homohopane index = [C_{35} 17α(H),21β(H)-homohopanes (22*S* + 22*R*) / ∑ $C_{31\text{-}35}$ 17α(H),21β(H)-homohopanes (22*S* + 22*R*)] x 10

The pristane/phytane ratio (Pr/Ph), a commonly used indicator of source redox conditions (Powell and McKirdy, 1973), varies between 1.1 and 1.4 in the asphaltite sample suite, suggesting that their source rock was deposited under sub-oxic conditions. However, their high C_{35} homohopane index values (7–9) and high sulphur content (≈ 4 wt. %) are consistent with more reducing conditions. The Pr/Ph ratios of the asphaltic tars are consistently lower, suggesting anoxia (<1; Table 1). This evidence of anoxia is further supported by a higher abundance of C_{35} homohopanes, expressed by high values of the C_{35} homohopane index (10–12) and C_{35}/C_{34} hopane ratio (1.00–1.05). Despite the evidence of a more oxygen-depleted (anoxic) setting (cf. the conflicting sub-oxic to anoxic parameters of the asphaltites), the sulphur content of the asphaltic tars varies between 2.5 and 3.5%, which is generally lower than that of the asphaltites (viz. 3.6–4.4% in the analysed suite).

The lithofacies of the asphaltite's source rock has previously been interpreted as a shale containing little to no carbonate, based on their C_{29}/C_{30} αβ hopane ratio being < 1 (Fig. 4, Table 1), their high relative abundance of diasteranes and the complete absence of 2α-methylhopanes (Edwards et al., 1998). Abundant 2α-methylhopanes are observed in oils derived from carbonate source rocks (Summons et al., 1999), while lower abundances are reported in deeper water facies, a trend attributed to the distribution of their precursor cyanobacteria which predominantly reside in shallow-water ecosystems (Eigenbrode et al., 2008). The unusual absence of 2α-methylhopanes in the asphaltites could therefore support the interpretation that the source rock was deposited in a deepwater setting, consistent with their complete lack of molecular markers indicating terrestrial or freshwater organic matter inputs.

Unlike the asphaltites, the asphaltic tars contain 2α-methylhopanes in low abundance. However, the significance of their presence is uncertain, as 2α-methylhopanes appear to require cracking from kerogen and are hence strongly affected by burial temperature (Peters et al. 2005). Additionally, the 17α-22,29,30-trisnorhopane (Tm) occurs in much higher abundance relative to the 18α-22,29,30-trisnorneohopane (Ts). These compounds are usually compared in the Ts/(Ts+Tm) ratio, which is commonly employed as a thermal

maturity parameter (Seifert and Moldowan, 1978). However, the low values of this ratio obtained from the asphaltic tars (0.19–0.27) are inconsistent with other thermal maturity parameters which indicate that these samples originated from the late oil window (discussed in Section 3.3). In addition to thermal maturity, the relative influence of lithology and redox conditions of the source rock on the Ts/(Ts+Tm) ratio is not fully understood, with several studies reporting systematically lower values in oils derived from carbonate source rocks deposited under anoxic conditions (McKirdy et al., 1983, 1984; Rullkötter et al., 1985; Price et al., 1987). Aside from this anomalous parameter, the composition of the asphaltic tars appears consistent with their derivation from an anoxic shale. To explain their abnormal Ts/(Ts+Tm) values, we tentatively propose that the source rock composition has a relatively high carbonate content, lying between the endmembers of shale and carbonate (i.e. a calcareous shale). In an anoxic setting, this may have been sufficient to account for their unusually low Ts/(Ts+Tm) values, despite the high thermal maturity of the parent oil.

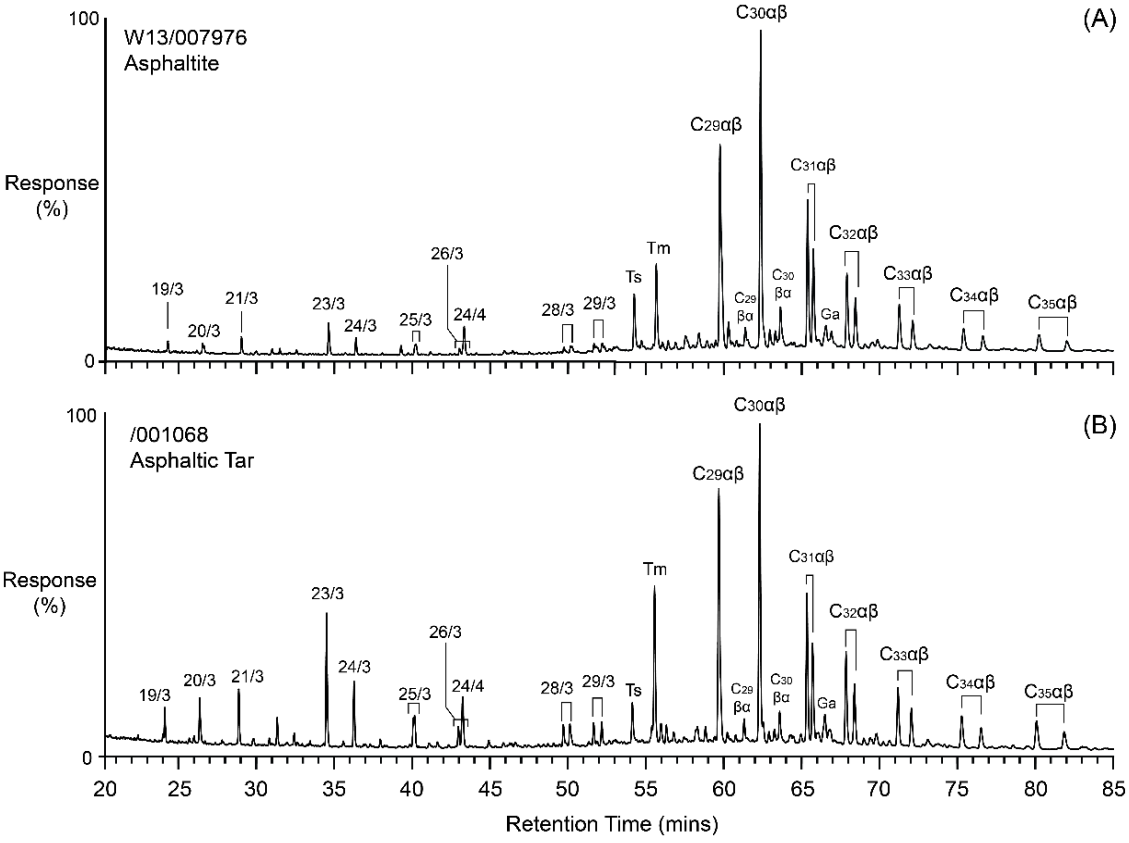

Figure 4: Partial *m/z* 191 chromatograms of (A) asphaltite sample W13/007976; and (B) asphaltic tar sample /001068. See Supplementary Information for full list of compound abbreviations.

3.2. Comparison of stable isotopic composition

The overall similarity of the asphaltic tars and asphaltites indicated by their near-identical source-specific sterane compositions is further reinforced by their internally consistent *n*-alkane $\delta^{13}C$ profiles, a valuable tool in the geochemical correlation of crude oils (e.g. Murray et al., 1994; Dowling et al., 1995; Blevin et al., 1998). The carbon isotopic composition of individual hydrocarbons in a crude oil is controlled principally by the primary organic matter inputs to its source rock. Hence oils derived from similar sources share comparable compound-specific $\delta^{13}C$ values (Hayes et al., 1990; Murray et al., 1994). The *n*-alkane $\delta^{13}C$ profiles of representative asphaltites and asphaltic tars, and of selected examples of Indonesian-derived waxy bitumens which also strand on the South Australian coastline (Ross et al., 2017) are shown in Figure 5. The isotopic values for each individual *n*-alkane in these specimens are listed in Table S2. The waxy bitumens, products of distal petroleum systems with source characteristics notably different to those of the asphaltites (cf. Edwards et al., 2018), contain C_{15+} *n*-alkanes with $\delta^{13}C$ values ranging between approximately –25.5 and –32‰. These results align with those of a previous assessment of the waxy bitumens' *n*-alkane isotopic composition, which demonstrated their similarity to the Minas and Duri oils from the Central Sumatra Basin (Dowling et al., 1995). In contrast, the *n*-alkane $\delta^{13}C$ values of the asphaltites and asphaltic tars are more uniform, with values between –30 and –34‰. Similarly, flat *n*-alkane $\delta^{13}C$ profiles are observed in other oils derived from marine source rocks (Murray et al., 1994).

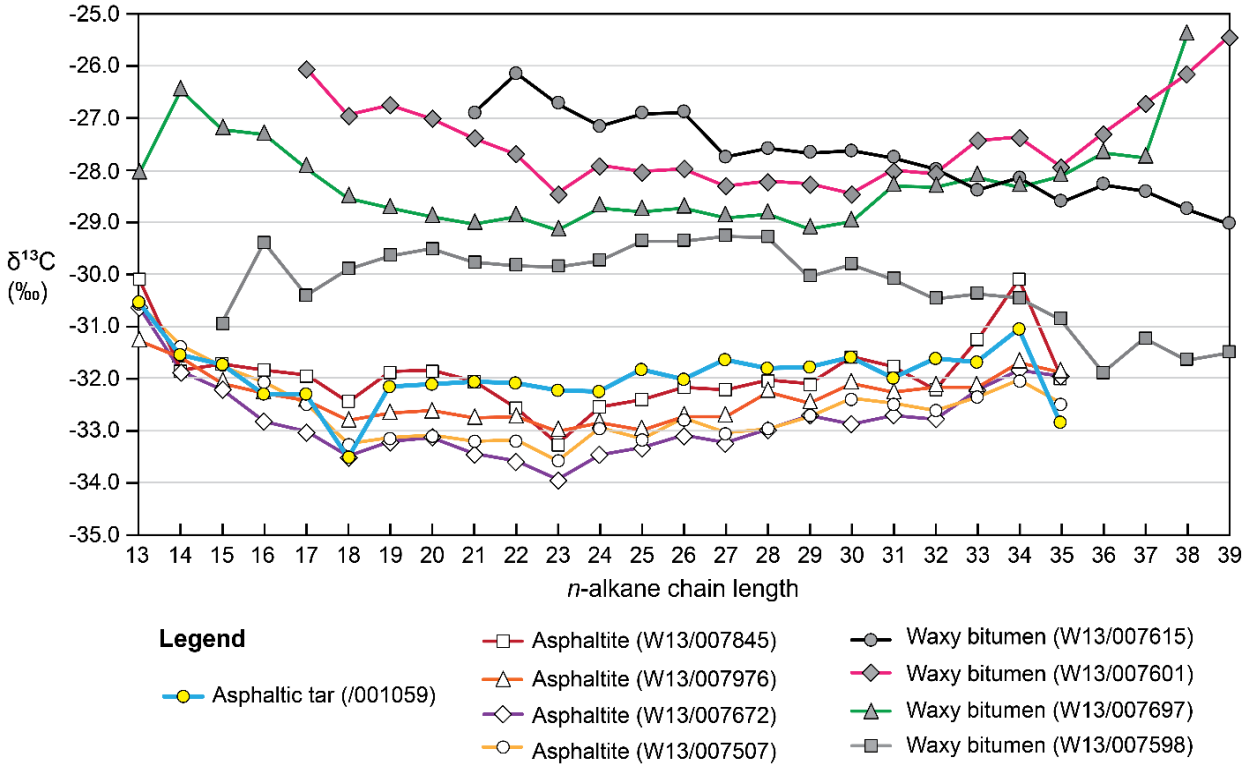

Figure 5: CSIA data on *n*-alkanes from interior subsamples of different coastal bitumen oil families collected from the South Australian coastline. The carbon isotopic profile of the asphaltic tar specimen plots in the same region as those of numerous asphaltites but differs markedly from those of waxy coastal bitumens derived from petroleum systems in Southeast Asia. Each of the waxy bitumen varieties shown are derived from different oil families identified using the presence/absence and abundance of key biomarker alkanes identifiable using whole-oil GC-MS (Corrick et al., 2016; Ross et al., 2017).

Although the carbon isotopic values of the two oil families are highly consistent, their bulk sulphur isotopic compositions ($\delta^{34}S$) differ considerably. The $\delta^{34}S$ signature of an oil may be used to aid oil-oil and oil-source correlations, as the unaltered value typically reflects that of the source kerogen (Thode et al., 1961; Thode and Monster, 1970; Orr, 1986). Although the primary source of the sulphur in marine organic matter is seawater sulphate, the process of bacterial sulphate reduction in the sediment prior to deeper burial results in organically-bound sulphur becoming depleted in ^{34}S (Jones and Starkey, 1957; Harrison and Thode, 1958; Thode et al., 1960). Hence, the $\delta^{34}S$ values of petroleum generated from this organic matter are typically ca. 15‰ lighter than contemporaneous inorganically precipitated sulphur minerals such as gypsum, which may either accurately preserve the composition of seawater or be enriched in ^{34}S (Thode and Monster, 1965). In asphaltites, bulk $\delta^{34}S$ values range between -3.6 and -4.6‰, while the values for the asphaltic tars are between +2.61 and +4.85‰, reflecting a much greater enrichment in the heavier isotope (Table 1). Given

the variability in the $\delta^{34}S$ composition of seawater sulphate during the Cretaceous, these heavier values remain geologically reasonable (cf. Paytan et al., 2004). However, the sulphur isotopic composition of crude oil may also be altered to heavier values under certain conditions (discussed in Section 4.2).

3.3. Comparison of thermal maturity parameters

The maturity parameters of the asphaltite and asphaltic tar samples are summarised in Table 2. As discussed previously, although the Ts/(Ts+Tm) ratio may often constrain thermal maturity, it is unreliable in this case due to likely source interference. The methylphenanthrene index (MPI-1), arguably the most robust molecular measure of thermal maturity (Radke, 1987), varies between 0.49 and 0.62 across the asphaltite samples. Using the relationship between MPI-1 and vitrinite reflectance defined by Radke and Welte (1983), the calculated vitrinite reflectance (R_c) of the asphaltites' source rock falls between 0.7 and 0.8%, indicating a thermal maturity in the early/main oil window, consistent with previous studies (Volkman et al., 1992; Edwards et al., 1998; Hall et al., 2014; Scarlett et al., 2019). Other aromatic maturity indices, namely the methylnaphthalene ratio (MNR) and dimethylnaphthalene ratio (DNR-1), yield slightly higher maturities in the range 0.9–1.0% R_c. This may be the result of mixing with a more mature oil charge, which will influence the methylnaphthalenes of the oil more than the higher-molecular-weight methylphenanthrenes.

The asphaltites used for comparison in this study were collected from widely separated stranding locations along the coastline (Fig. 1A) and, with few exceptions, preserve phenanthrene, comparable to those in previous studies (cf. Volkman et al., 1992; Edwards et al., 1998; Hall et al., 2014). Therefore, most asphaltites within the sample suite have undergone minimal alteration due to water-washing, supporting the interpretation that they are the product of a local seafloor seep (Hall et al., 2014). However, degraded asphaltites do occur (e.g. samples W13/007493 and W13/007668). Such mild to moderately degraded examples exhibit significant alteration to the methyl- and dimethylnaphthalenes, while the MPI-1 ratio appears relatively unaffected (Corrick et al., 2019).

Table 2: Thermal maturity parameters and calculated vitrinite reflectance (R_c) values of asphaltites and asphaltic tars. MPI-1 ratio after Cassani et al. (1988). Relationship between MPI-1 and R_c after Radke and Welte (1983). MNR, DNR-1 ratios and their respective relationships to R_c after Radke et al. (1984). See Supplementary Information for all compound abbreviations.

Sample	Tricyclics / 17α-hopanes	MPI-1	R_c (%) from MPI-1	MNR	R_c (%) from MNR	DNR-1	R_c (%) from DNR-1
Asphaltites							
W13/007472	0.08	0.49	0.7	0.63	0.9	2.57	1.0
W13/007475	0.10	0.62	0.8	0.75	0.9	2.20	1.0
W13/007476	0.09	0.51	0.7	0.81	1.0	2.39	1.0
W13/007488	0.09	0.49	0.7	0.81	1.0	2.20	1.0
W13/007493	0.07	0.60	0.8	*	*	*	*
W13/007507	0.12	0.49	0.7	0.98	1.0	2.43	1.0
W13/007516	0.10	0.53	0.7	0.72	0.9	2.46	1.0
W13/007668	0.11	0.61	0.8	*	*	*	*
W13/007671	0.10	0.55	0.7	0.72	0.9	2.31	1.0
W13/007672	0.10	0.53	0.7	0.77	1.0	2.31	1.0
W13/007845	0.15	0.51	0.7	0.83	1.0	2.58	1.0
W13/007976	0.11	0.54	0.7	0.93	1.0	2.98	1.0
Asphaltic Tars							
/001056	0.31	1.28	1.2	1.76	1.1	6.82	1.2
/001063	0.33	1.26	1.2	1.73	1.1	7.22	1.2
/001067	0.31	1.23	1.1	1.66	1.1	7.10	1.2
/001068	0.34	1.25	1.1	1.59	1.1	6.24	1.2
/001076	0.24	1.33	1.2	1.62	1.1	6.07	1.2
/001079	0.26	1.34	1.2	1.71	1.1	7.29	1.2
/001081	0.27	1.31	1.2	1.55	1.1	6.42	1.2

* Ratio altered due to significant water washing and removal of key aromatic compounds.
Tricyclics/17α-hopanes = $\sum C_{19\text{-}30}$ tricyclic terpanes / $\sum C_{29\text{-}35}$ αβ hopanes
MPI-1 = [1.89 x (2-MP + 3-MP)] / [P + 1.26 (1-MP + 9-MP)]
R_c (%) from MPI-1 = 0.60 x MPI-1 + 0.40
MNR = 2-MN / 1-MN
R_c (%) from MNR = 0.17 x MNR + 0.82
DNR-1 = (2,6-DMN + 2,7-DMN) / 1,5-DMN
R_c (%) from DNR = 0.046 x DNR-1 + 0.89

The aromatic hydrocarbon fraction of the asphaltic tars differs notably from that of the asphaltites (Fig. S2, Table 2). Their MPI-1 values of 1.23–1.34 are equivalent to R_c values of 1.1–1.2%, indicating a thermal maturity within the late oil window. MNR and DNR-1 likewise yield R_c values of 1.1 and 1.2% respectively. This consistency between aromatic maturity indicators suggests the asphaltic tars are unlikely to represent a mix of earlier and later expulsion products (*c.f.* the higher R_c values from MNR and DNR-1 vs. MPI-1 in the asphaltites). Like the asphaltites, the preservation of somewhat water-soluble naphthalenes, despite exposure to the marine environment, supports the interpretation that the asphaltic tars also originated from a nearby petroleum system.

458

459 The abundance of tricyclic terpanes relative to 17α-hopanes has been shown to increase at
460 higher thermal maturities due to the preferential release of tricyclic terpanes from kerogen
461 (Aquino Neto et al., 1983; van Graas, 1990; Farrimond et al., 1999). The tricyclic
462 terpanes/17α-hopanes ratios of the asphaltites are low (0.07–0.15), consistent with their
463 other maturity parameters which suggest generation and expulsion from a source rock in
464 the early oil window. The markedly higher thermal maturity of the asphaltic tars indicated
465 by their aromatic maturity parameters is further supported by their higher tricyclic
466 terpanes/17α-hopanes ratio of 0.24–0.34 (Table 2). However, the abundance and
467 composition of tricyclic and tetracyclic terpanes can also reflect source input (Peters et al.,
468 2005). This makes distinguishing the influence of source and thermal maturity difficult when
469 comparing two oils of markedly different maturities.

470

471 *3.4. Comparison of Re-Os systematics*

472 The Re-Os geochronology of crude oils has been demonstrated to constrain the timing of oil
473 generation and expulsion from the source rock (Selby et al., 2005; Selby and Creaser, 2005;
474 Finlay et al., 2011; Lillis and Selby, 2013; Liu et al., 2018). Application of the Re-Os
475 geochronometer to asphaltites recently collected from the South Australian coastline
476 provided a generation age of 74 ± 26 Ma (n =16; Corrick et al., 2019), while analysis of a
477 smaller suite of archival specimens collected in the 1990's yielded a set of data points with
478 lower analytical uncertainty which define an age of 103 ± 22 Ma (n = 5; Scarlett et al., 2019).
479 These generation ages show 19 Myr of potential overlap when considering their respective
480 uncertainties. However, the remaining variation between these two determined ages is
481 unlikely to be soley attributable to the differences in analytical uncertainty between these
482 two studies, as the results obtained from numerous asphaltites analysed by Corrick et al.
483 (2019), despite their higher analytical uncertaintly, do not overlap with, or plot along the
484 isochron defined by Scarlett et al. (2019). This suggests that a geologic component to the
485 variation is also likely. The overall high uncertainty present in both of the determined ages
486 may be associated with the mixing of increasingly mature oil, given the variation observed
487 between the aromatic maturity parameters used herein (Table 2).

The asphaltic tars contain 30.1–31.4 parts per billion (ppb) Re and 599.9–627.6 parts per trillion (ppt) Os, concentrations significantly greater than in the asphaltites, which contain between 2.6-4.2 ppb Re and 24.6-45.0 ppt Os (Corrick et al., 2019; Scarlett et al., 2019). Such high abundances of Re and Os are unusual, particularly as these elements predominantly reside within the asphaltene fraction of crude oil (Selby et al., 2007; Georgiev et al., 2016; Liu and Selby, 2018; Liu et al., 2019) and the asphaltic tars contain less asphaltenes (22–35% versus 51–59% in the asphaltites; Table 1). The $^{187}Re/^{188}Os$ and $^{187}Os/^{188}Os$ ratios of the analysed asphaltic tars are highly uniform at 332.2–333.9 and 3.057–3.063, respectively (Table S3). These values overlap when considering the range of analytical uncertainty. Thus, insufficient variation exists to apply a linear regression to these data points to determine a meaningful generation age for the asphaltic tars. Their homogenous Re and Os composition is likely due to both the small number of samples analysed (n = 3), and the high probability that the specimens analysed represent individual fragments of a single larger piece of tar, as discussed previously. Whilst internally consistent, these values differ from those obtained from the asphaltites (Fig. 6), which yield $^{187}Re/^{188}Os$ values between 400.5–547.8 and $^{187}Os/^{188}Os$ values of 1.122–1.334 (Corrick et al., 2019; Scarlett et al., 2019).

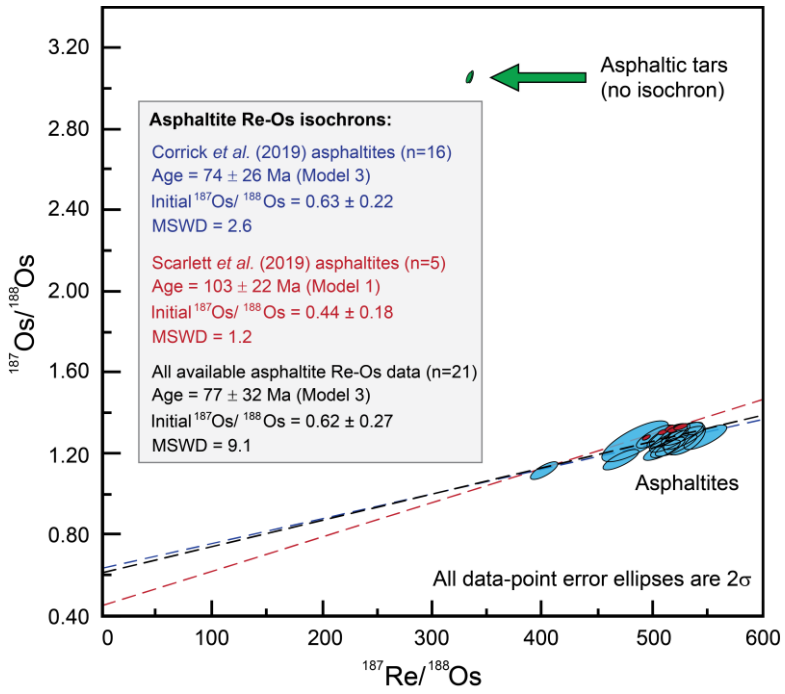

Figure 6: Comparison of Re-Os ratios of asphaltic tars with those of asphaltites analysed by Corrick et al. (2019) and Scarlett et al. (2019). Results for individual samples are listed in Table S3. MSWD = mean square of weighted deviates.

4. DO BOTH OILS ORIGINATE FROM THE SAME SOURCE ROCK?

The geochemistries of these two varieties of asphaltic crude oil exhibit several source-related similarities, such as their highly comparable sterane distributions and *n*-alkane $\delta^{13}C$ values. However, clear and systematic differences are also evident between these two oil types, most notably in their respective Ts/(Ts+Tm) ratios, bulk $\delta^{34}S$ values and Re-Os systematics. Oil-oil and oil-source correlations can become particularly complex when taking into account possible lateral variations in both the organic facies and thermal maturity of the source rock. Therefore, the relationship between these two oil types must be considered in terms of two competing interpretations: (1) The asphaltic tars and asphaltites were derived from separate source rocks which contained similar organic facies; or (2) both oil types originated from lateral equivalents of the same source rock unit. In the latter interpretation, the observed geochemical variations reflect minor lateral variability in the source rock composition, combined with increased thermal maturity and possible alteration by thermochemical sulphate reduction (TSR; discussed below).

In both scenarios, correlation of the two oil types based on multiple source-specific parameters supports their derivation from organic-rich rocks which contained highly comparable organic matter inputs. Thus, these two asphaltic oils are likely to have originated from within the same basin, presently considered to be the offshore Bight Basin. However, the implications of the two potential interpretations for the quality and location of the asphaltic tars' parent petroleum system may differ considerably.

4.1. The case for two separate source rocks

Multiple marine intervals with high source potential are proposed to occur throughout the Blue Whale, White Pointer, Tiger and Hammerhead supersequences of the Bight Basin (Blevin et al., 2000; Totterdell et al., 2000; Struckmeyer et al., 2001; Totterdell et al., 2008); and many of these now lie within different stages of the hydrocarbon generation window, depending on their location. For example, in the depocentre of the Ceduna Sub-basin, the proposed source rocks in the Blue Whale and White Pointer supersequences reside in the gas window or overmature zones, while laterally these intervals pass through both the main and late oil window in both the marginal and basinward areas (Fig. 7). It is reasonable to consider that organic matter inputs to a marine sedimentary basin would be similar, though not necessarily identical through time. An interpretation of two discrete marine source rock intervals with similar organic matter inputs would permit the near-identical compound-specific $\delta^{13}C$ values and sterane distributions of the asphaltites and asphaltic tars. However, the observed differences in $\delta^{34}S$ values and Re-Os systematics may be attributed to variations of seawater chemistry through time (e.g. Paytan et al., 2004; Du Vivier et al., 2014). Although this may account for different $^{187}Re/^{188}Os$ and $^{187}Os/^{188}Os$ values between the two oils, it does not explain the unusually high abundance of Re and Os present in the asphaltic tars. Whilst the possibility of two separate sources cannot be discounted, this interpretation relies predominantly on attributing all observed variations between these two asphaltic oil strandings to differences in source rock composition, with little to no acknowledgement of the role that lateral facies variation and differing thermal maturity may also have had on the composition of the oil generated throughout the basin.

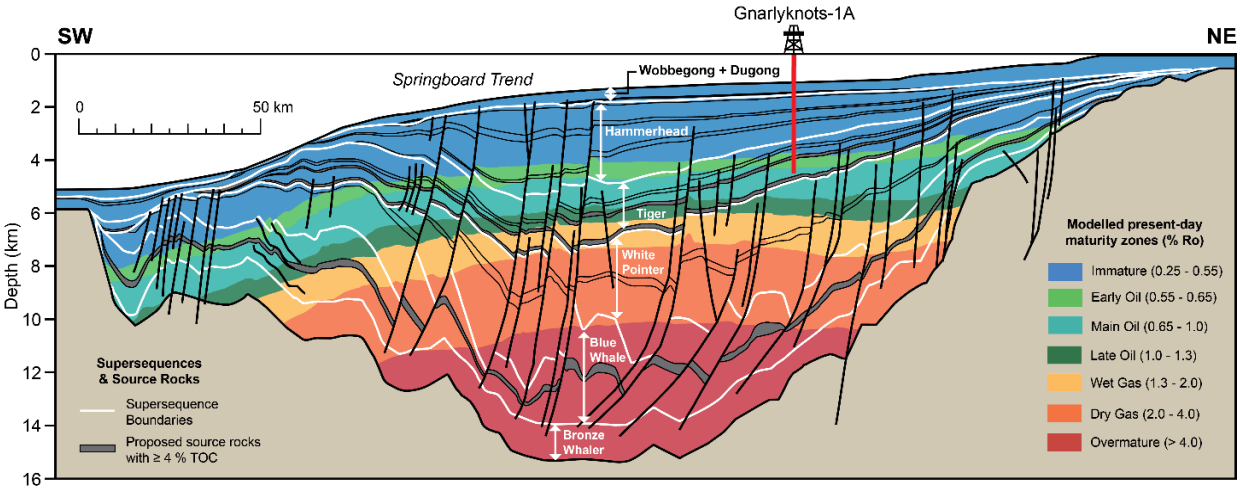

Figure 7: Cross-section of the Ceduna Sub-basin of the Bight Basin with supersequence boundaries, proposed source intervals (> 4% TOC) and modelled present-day maturity (% R_o) zones. Figure modified after Totterdell et al. (2008).

4.2. The case for a single source rock

The geochemical differences between the asphaltic tars and asphaltites may also be attributed to a combination of minor lateral variation in source rock facies, differences in thermal maturity and alteration of the asphaltic tars by TSR. This latter process occurs when oil comes into contact with a source of dissolved sulphate at temperatures at or above 100–140°C (Goldhaber and Orr, 1995; Machel, 2001). Potential sources of dissolved sulphate include buried seawater, basin brines (groundwater) or dissolved evaporite deposits of gypsum or anhydrite (Machel, 2001). During TSR, low-molecular-weight hydrocarbons are oxidised in order to reduce the dissolved sulphate. Branched and *n*-alkanes are the most reactive, followed by cyclic and monoaromatic compounds (Krouse et al., 1988; Manzano et al., 1997; Machel, 2001). Products of this reaction include hydrogen sulphide (H_2S), carbonate, metal sulphides and pyrobitumen (Machel, 2001). The release of H_2S in particular can also have important technical implications for oil production, as the oxidation reduces the overall hydrocarbon potential and production costs are increased due to the toxicity of H_2S and its associated corrosion of drilling equipment.

Both the sulphur isotopic composition and Re-Os systematics of a crude oil, two parameters typically inherited from seawater at the time of source rock deposition, are severely altered

during TSR. Alteration of primary $\delta^{34}S$ values occurs due to the back reaction of the resulting H_2S with the oil. This incorporates sulphur derived from the dissolved sulphate, driving the $\delta^{34}S$ composition towards heavier values (e.g. Orr, 1974; Lillis and Selby, 2013). This is consistent with the observed difference in $\delta^{34}S$ composition between the asphaltic tars and asphaltites (Table 1). TSR has also been observed to reset the Re-Os systematics of crude oils, with the resulting age representing the cessation of this alteration process (Lillis and Selby, 2013). Oils affected by TSR are enriched in both Re and Os relative to the parent oil and possess different $^{187}Re/^{188}Os$ and $^{187}Os/^{188}Os$ ratios (Lillis and Selby, 2013). This suggests that during TSR both Re and Os are also transferred from the dissolved sulphate phase to the oil, though the exact nature of this process remains unclear. The resulting $^{187}Re/^{188}Os$ and $^{187}Os/^{188}Os$ values of the oil will therefore represent mixed signatures of the original oil and the dissolved sulphate. The nature of this alteration is unlikely to be systematic in all cases (i.e. $^{187}Os/^{188}Os$ will not always increase), as the composition of the dissolved sulphate will vary in different settings according to the sources of Re and Os (e.g. balance of Re and Os derived from mantle inputs vs. continental weathering). Disruption of the Re-Os systematics due to TSR is consistent with the differences observed between the asphaltites and asphaltic tars. In particular, the significant enrichment of both Re and Os in the latter, despite their lower asphaltene content. Although the asphaltic tars lacked the necessary variation to produce a meaningful isochron, it is likely that their Re-Os systematics actually constrain the cessation of TSR. Hence, their marked departure from those of the asphaltites, which are considered to record a generation age (Corrick et al., 2019; Scarlett et al., 2019).

A second potential explanation for resetting Re-Os systematics is oil-water interaction without TSR. Laboratory experiments have also shown Re and Os may be rapidly transferred to liquid oil when in contact with a solution enriched in Re and Os (Mahdaoui et al., 2015; Hurtig et al., 2019). Though these studies cannot fully mimic natural oil-water interactions in a geologic setting, their results suggest that interaction of oil with formation waters, which contain much lower abundances of Re and Os, may be capable of altering and resetting the Re-Os composition of an oil, given sufficiently high water/oil ratios (ca. 250). In this case, such formation waters would require highly radiogenic Os in order to alter the $^{187}Os/^{188}Os$ ratios of the asphaltic tars to their observed values (3.057–3.063), which are much higher

than those reported for the asphaltites (1.122–1.334: Corrick et al., 2019; Scarlett et al., 2019). However, the influence of basinal water on the Re-Os systematics of crude oils and their application to constraining the timing of generation has been demonstrated to be limited or negligible in the Duvernay petroleum system of the West Canada Sedimentary Basin (Liu et al., 2018) wherein certain oils contain very low concentrations of both Re (0.04–3.78 ppb) and Os (0.6–41.2 ppt). Such examples should be extremely sensitive to any Re-Os contamination, but such alteration is not observed. Therefore, overprinting from typical interaction with formation waters is unlikely, given the evidence supportive of their alteration by TSR.

Definitive identification that a crude oil has been altered by TSR typically requires identification of thiaadamantanes (Wei et al., 2012), or a combination of evidence from obtained from complementary analyses, notably assessment of the resulting gases (H_2S and CO_2), low-molecular-weight hydrocarbons and precipitated phases including carbonates, pyrobitumens and metal sulphides (e.g. Machel et al., 1995; Machel, 2001; Li et al., 2005; Hao et al., 2008; Liu et al., 2016). Unfortunately, the asphaltic tars do not appear to contain any compounds with mass spectra consistent with thiaadamantane or its various methylated homologues. However, if thiaadamantanes were originally present, they would likely have been lost along with the other low-molecular-weight hydrocarbons due to weathering in the marine environment. Therefore, without fresh examples for comparison, the absence of thiaadamantanes does not definitively preclude TSR in this case. Furthermore, as these oils were collected from the coastline, complementary analyses of the other products of TSR discussed above are not available for comparison as the location of the reservoir is not known. Given this ambiguity, we cannot conclusively determine that TSR has altered the asphaltic tars, although we note it would be consistent with their bulk $\delta^{34}S$ values and Re-Os systematics. Analysis of these oils in a more concentrated form using GC-MS-MS targeting the 2-thiaadamantane and the methlated thiaadamantanes may be able to assess this interpretation further. Alternatively, comparison of the compoud-specific sulphur isotopic composition of the benzothiophenes and dibenzothiophenes may also be diagnostic (Amrani et al., 2012).

642 The other noted differences between the asphaltites and asphaltic tars are consistent with
643 minor lateral variation in organic facies and the expulsion of the latter from the source rock
644 later in the oil generation window. The carbonate content and redox conditions of a source
645 rock formation may vary laterally across a basin due to its proximity to shallow water
646 carbonate systems and variations in seafloor topography beneath a stratified water column,
647 respectively. Such variability would be consistent with the minor variations in redox
648 parameters (e.g. Pr/Ph, C_{35} homohopane index) between the two oil types and a calcareous
649 shale source for the asphaltic tars, as indicated by their unusually low Ts/(Ts+Tm) values for
650 an oil generated in the late oil window. The higher thermal maturity of the asphaltic tars is
651 also consistent with their greater abundance of tricyclic terpanes relative to hopanes when
652 compared to the asphaltites. Finally, both increasing thermal maturity and TSR are known to
653 affect the $\delta^{13}C$ composition of the oil. Mature oils contain individual low-molecular-weight
654 hydrocarbons which are 1–3‰ more enriched in ^{13}C relative to their less mature
655 equivalents, while alteration by TSR results in even greater enrichment (> +15‰: Rooney,
656 1995). The light hydrocarbons affected by these processes are not preserved in the asphaltic
657 tars, and therefore neither of these diagnostic changes can be assessed based on the
658 isotopic composition of their C_{13}–C_{35} *n*-alkanes (Fig. 5).

659

660 In summary, whilst the differences between the asphaltites and asphaltic tars could be
661 attributted to their derivation from separate source rocks, the specific points of variation
662 are also consistent with the latter's higher thermal maturity, alteration by TSR and minor
663 lateral variation in source facies (Table 3).

664

665

666

667

668

669 **Table 3: Summary of processes capable of creating the observed geochemical differences between the**
670 **asphaltic tars and asphaltites under the single source rock interpretation.**

Deviation from asphaltite geochemistry	*Potential mechanisms*
(1) Higher abundance of tricyclic terpanes relative to hopanes	• Preferential expulsion of terpanes from kerogen at higher thermal maturities (Aquino Neto et al., 1983; van Graas, 1990; Farrimond et al., 1999)
(2) Lower sulphur content	• Lateral variability in euxinic conditions across basin • Thermal decomposition of organosulphur compounds in oil to gases (Orr, 1974; Tissot and Welte, 1984)
(3) Heavier $\delta^{34}S$ values	• Uptake of sulphur from dissolved sulphates and/or back reaction of H_2S during TSR (Orr, 1974; Lillis and Selby, 2013)
(4) Enriched Re and Os abundance and highly different Re-Os ratios	• Alteration due to TSR (Lillis and Selby, 2013)
(5) Pr/Ph < 1	• Lateral variability of source rock redox conditions
(6) Minor variation in C_{29}/C_{30} αβ hopane ratio	• Minor lateral variability in source rock carbonate content • Preferential thermal degradation of C_{30} αβ hopane (Peters et al., 2005)
(7) Presence of 2α-methylhopanes	• Minor increase in carbonate content • Increased thermal maturity
(8) Lower Ts / (Ts+Tm)	• Greater relative abundance of Tm attributed to higher carbonate content and anoxic conditions rather than thermal maturity (e.g. McKirdy et al., 1983, 1984; Rullkötter et al., 1985; Price et al., 1987)

671

672

673 ## *4.3. Potential mechanisms of heavy petroleum formation*

674 Naturally occurring viscous tars/bitumen may form in response to a variety of different
675 processes. These include: (1) extensive biodegradation of crude oil in a shallow subsurface
676 reservoir; (2) weathering and amalgamation of a sea-surface oil slick, leaving a viscous
677 residue which may be subsequently separated by wave action (Logan et al., 2010; Warnock
678 et al., 2015); (3) *in situ* thermal maturation of a crude oil resulting in the formation of
679 pyrobitumen (Machel, 2001); (4) separation of heavy petroleum to form subsurface tar
680 mats, which may occur in several different ways (Dahl and Speers, 1986; Wilhelms and
681 Larter, 1994a, 1994b); and (5) direct seepage of heavy petroleum onto the seafloor (e.g.
682 Brüning et al., 2010), where it then becomes immobile.

683

684 Many of these potential mechanisms are inconsistent with the composition of the asphaltic
685 tars and may therefore be discounted. Firstly, although they have a slightly lower *n*-alkane

686 content than the freshest examples of asphaltite, the asphaltic tars do not appear to be
687 heavily biodegraded, as they still contain C_{10+} *n*-alkanes. The preservation of the somewhat
688 water-soluble naphthalenes in the least altered asphaltites and the entire suite of asphaltic
689 tars also suggests that, despite their interaction with seawater, water washing has not been
690 extensive. This likely precludes their formation from the weathering and amalgamation of
691 an oil slick, whether from a spilled oil or natural seepage. Liquid oil in seawater will disperse
692 into a thin surface slick with an extremely high surface area to volume ratio, making the oil
693 extremely vulnerable to water washing, oxidation and microbial action. Generally, such oil in
694 the marine environment will lose the majority of its low-molecular-weight components in a
695 matter of hours (Head et al., 2006). Additionally, other known examples of marine tars
696 amalgamating from sea surface oil slicks notably required calm oceanic conditions to form
697 (e.g. Lorenson et al., 2009). The high energy environment of the Great Australian Bight,
698 including the intense storm which occurred prior to the collection of the asphaltic tars, is
699 unlikely to be supportive of this process.

700

701 *In-situ* thermal maturation of reservoired crude oil or alteration by TSR are known to form
702 pyrobitumen. These solid residues are only weakly soluble in organic solvents (Wilhelms and
703 Larter, 1994b) and are unlikely to seep. Previous assessment of their origin by Hall et al.
704 (2014) demonstrated that the asphaltites are not pyrobitumen as they readily dissolve in
705 dichloromethane. Although the asphaltic tars were generated and expelled during the late
706 oil window, they are similarly soluble in dichloromethane and therefore they, too, cannot be
707 considered residues of thermal maturation.

708

709 Hall et al. (2014) proposed that the asphaltites are transported remnants of subsurface tar
710 mats, also known as viscous oil zones, polar-enriched zones (Larter et al., 1990) or heavy oil
711 tar zones (Haldorsen et al., 1985). These deposits of heavy petroleum are reported in both
712 clastic and carbonate settings and may range in thickness from <1 m to as much as 6 m
713 (Larter et al., 1990; Wilhelms and Larter, 1994a, 1994b). Well characterised examples
714 demonstrate these emplacements of heavy petroleum share comparable biomarker
715 geochemistry with their parent oils but are more enriched in asphaltenes (20–60 wt %; cf.

716 1–5 wt % in the oil leg: Wilhelms and Larter, 1994a, 1994b). Tar mats are readily soluble in
717 organic solvents, clearly distinguishing them from weakly soluble pyrobitumen formed
718 during reservoir maturation (Milner et al., 1977; Wilhelms and Larter, 1994a). These
719 deposits may separate from the main oil charge in response to several different processes,
720 including gravity segregation, introduction of gas to the reservoir and decreasing reservoir
721 pressures, or are due to permeability barriers (Milner et al., 1977; Dahl and Speers, 1986;
722 Wilhelms and Larter, 1994a, 1994b). In particular, deasphalting of the oil in response to gas
723 generation from a maturing reservoired oil could account for the formation of the asphaltic
724 tars, given that their thermal maturity (R_c = 1.1–1.2%) lies at the boundary of the wet gas
725 window (R_c = 1.3%). Migration of gas into the reservoir is also possible, given the faulting
726 which may connect to regions of the basin in the gas window (Fig. 7). However, ultimately
727 none of the processes listed above can be discounted, as the resulting heavy petroleum in
728 each case displays no diagnostic changes to its geochemistry. A more detailed knowledge of
729 the geologic context of their parent petroleum system is therefore required to assess these
730 mechanisms further.

731

732 Considering the asphaltic tars and asphaltite strandings as pieces of previously emplaced tar
733 mats is also problematic, as it also requires facilitating their migration to the seafloor,
734 despite their tendency to remain in place in the subsurface. Hall et al. (2014) suggested that
735 following their formation as tar mats, the asphaltites escaped the subsurface by way of
736 submarine canyon incision. However, it is more likely that seepage of both the asphaltites
737 and the asphaltic tars is analogous to the asphalt flows observed on the seafloor in the Gulf
738 of Mexico (Brüning et al., 2010). In this case, heavy petroleum that has not yet become
739 immobile reaches the seafloor in a viscous state and flows away from the seepage site. The
740 loss of volatile components, oxidation and other processes progressively increases the
741 viscosity of the oil to the point where it becomes immobile and ultimately solidifies. The
742 deposit forms deep fissures and cracks due to the loss of its low-molecular-weight
743 hydrocarbons. The bitumen eventually fragments, releasing material into the overlying
744 water column where it can become entrained in ocean currents. This process is certainly
745 consistent with the shrinkage cracks seen in the larger asphaltites (Fig. 1B). The asphaltic
746 tars, which have not solidified, may be more analogous to the seafloor tar mounds/whips

observed off the southern coast of Santa Barbara (Lorenson et al., 2009). In this case, however, the oil has not been extensively biodegraded like that encountered in the Santa Barbara seeps.

4.4. *Constraining the location of the asphaltic tar petroleum system*

The prior coastal surveys conducted in November 2014 and September 2015 found no examples of this new variety of asphaltic crude oil across the 30 systematically surveyed beaches (Ross et al., 2017). There are similarly no reports of any oil matching their geochemical signature in previous studies of Australian coastal bitumen (McKirdy, 1984a, 1984b; Currie et al., 1992; Volkman et al., 1992; Summons et al., 1993; Alexander et al., 1994; Padley, 1995; Edwards et al., 1998, Hall et al., 2014; Edwards 2016, 2018). The beach where the asphaltic tars were found, Number 1 and 2 Rocks, is also the most prominent collection point for coastal bitumen identified on the South Australian coastline (Padley, 1995; Edwards et al., 2016; Ross et al., 2017). Despite the abundance of coastal bitumen recovered from this site, no asphaltites were found there during the three annual surveys conducted in 2014–2016 (Ross et al., 2017), nor during the systematic bi-monthly surveys conducted in 1990 and 1991 (Padley, 1995; Edwards et al., 2016). However, it is important to acknowledge that the asphaltic tar strandings were collected just 24 days after a one-in-fifty-year storm event which affected much of the South Australian coastline (Bureau of Meteorology, 2016; Burns et al., 2017). The resulting abnormal wind and wave behaviour likely caused a significant departure from their traditional oceanic transport pathway and ultimate stranding location. Therefore, the single stranding location of the asphaltic tars presently provides little constraint on their point of origin.

If the asphaltic tars were derived from an oil affected by TSR then the parent oil must reside within a region of the subsurface which meets the required minimum onset temperature of 100–140° (Goldhaber and Orr, 1995; Machel, 2001). This may permit assessment of potential reservoirs based on the general increase in temperature with depth (e.g. Fig. 7). However, locally increased temperatures will also occur in proximity to volcanism and circulating hydrothermal fluids. The Bight Basin hosts an approximately 50,000 km^2 complex

777 of volcanic intrusions in the Ceduna Sub-basin and the overlying Eucla Basin, with isolated
778 igneous bodies also reported in the adjacent Duntroon Sub-basin (Schofield and Totterdell,
779 2008). Thus, circulating hydrothermal fluids could also provide the necessary temperatures
780 and dissolved sulphate for TSR to occur within shallower regions of the basin. This is further
781 supported by the recent identification of hydrocarbon-containing fluid inclusion
782 assemblages in the Duntroon Sub-basin which appear to have been altered by hydrothermal
783 fluids (Bourdet et al., *submitted*). However, no hydrocarbons extracted from fluid inclusions
784 in the Bight Basin have a composition consistent with the asphaltites or asphaltic tars
785 (Kempton et al., *submitted*; Gong et al., *submitted*).

786

787 Oils altered by TSR are primarily encountered in reservoirs with limited clay content such as
788 clean sandstones or carbonates, as the presence of iron within clay minerals will react with
789 available H_2S to form pyrite, rather than permitting it to accumulate to high concentrations
790 (Worden and Smalley, 2011; Machel, 2001). In order for TSR to occur in clastic sediments
791 containing clays, a larger source of dissolved sulphate is required (e.g. dissolved evaporite
792 deposits) to exhaust all of the available iron before H_2S can accumulate. Presently there are
793 no proposed carbonate reservoirs or evaporite deposits within the Bight Basin. Therefore, if
794 the asphaltic tars have been altered by TSR, the reservoir would likely reside within clean
795 sandstones deposited as part of the Ceduna delta, using sulphate sourced from
796 groundwaters or circulating hydrothermal fluids. However, as the evidence for alteration by
797 TSR is not conclusive, proposing an exact location for the parent petroleum system within
798 this frontier basin remains speculative.

799

800 5. CONCLUSIONS

801 A new type of stranded crude oil termed ‘asphaltic tar’ was encountered during coastal
802 surveys of South Australia in October 2016. These strandings share source-specific features
803 with the well-studied asphaltites, also found on the South Australian coastline. Thermal
804 maturity parameters constrain the asphaltic tar to the late oil window, unlike the asphaltites
805 which were generated within the early oil window. The contrasting thermal maturity of the
806 two oil types renders their correlation uncertain. Despite their source-specific similarities,

differences in several geochemical parameters of the two oil types suggest that each may have originated from separate source rocks with comparable marine organic matter inputs. However, the most prominent differences accord with the higher thermal maturity of the asphaltic tar and its alteration by thermochemical sulphate reduction. Both interpretations are consistent with these two oil types originating from within the same basin. As the asphaltites are presently attributed to an undiscovered petroleum system in the nearby Bight Basin, we consider these newly discovered asphaltic tars to have a similar origin.

ACKNOWLEDGEMENTS

CSIA data were collected by the Davis Isotope Laboratory, University of California. Re-Os data were collected at the Laboratory for Source Rock Geochronology and Geochemistry and Arthur Holmes Laboratory at Durham University (UK). A.J.C. acknowledges the financial support of the Bernold M. “Bruno” Hanson Memorial Environmental Grant from the AAPG Grants-In-Aid Program, The D R Stranks Travelling Fellowship, a University of Adelaide postgraduate scholarship and additional funding from the Great Australian Bight Research Program. D.S. acknowledges the Total Endowment Fund and the CUG Wuhan Dida Scholarship. We thank Zachary Angelini, Chris Dyt, Richard Kempton, Cameron White, April Pickard, Stacey Maslin, Stephane Armand, Les Tucker and Su Margot for their assistance in completing the 2014–2016 beach surveys. We also thank Mark Rollog and Robyn Williamson for conducting the EA-IRMS analyses; Antonia Hofmann and Geoff Nowell for assistance with the Re-Os determinations; and Stuart Valladares for the donation of asphaltites from his personal collection for this research. Finally, we thank Charlotte Stalvies, Chris Boreham, Herbert Volk and Jennifer Totterdell for their constructive feedback on our manuscript.

The Great Australian Bight Research Program is a collaboration between BP, CSIRO, the South Australian Research and Development Institute (SARDI), the University of Adelaide, and Flinders University. The program aims to provide a whole-of-system understanding of the environmental and social values of the region; providing an information source for all to use.

FUNDING

Fieldwork and analytical costs for the research were met by the Great Australian Bight Research Program. Further financial support for the acquisition of Re-Os data was provided by the Bernold M. “Bruno” Hanson Memorial Environmental Grant to A.J.C. as part of the AAPG Grants-In-Aid Program.

REFERENCES

Alexander, R., Currie, T.J., Kagi, R.I., 1994. The origins of coastal bitumens from Western Australia. Aust. Pet. Expor. Assoc. J. 34 (1), 787–798.

Amrani, A., Deev, A., Sessions, A.L., Tang, Y., Adkins, J.F., Hill, R.J., Moldowan, J.M., Wei, Z., 2012. The sulfur-isotopic compositions of benzothiophenes and dibenzothiophenes as a proxy for thermochemical sulfate reduction. Geochim. Cosmochim. Acta 84, 152–164. doi:10.1016/J.GCA.2012.01.023

Aquino Neto, F.R., Trendel, J.M., Restle, A., Connan, J., Albrecht, P.A., 1983. Occurrence and formation of tricyclic and tetracyclic terpanes in sediments and petroleum. In: Bjoröy, M., Albrecht, P., Cornford, C., de Groot, K., Eglinton, G., Galimov, E., Leythaeuser, D., Pelet, R., Speers, G. (Eds.), Advances in Organic Geochemistry 1981. John Wiley & Sons Limited, Chichester, pp. 659–676.

Bastow, T.P., van Aarssen, B.G.K., Lang, D., 2007. Rapid small-scale separation of saturate, aromatic and polar components in petroleum. Org. Geochem. 38, 1235–1250. doi:10.1016/j.orggeochem.2007.03.004

Blevin, J.E., Boreham, C.J., Summons, R.E., Struckmeyer, H.I.M., Loutit, T.S., 1998. An effective Lower Cretaceous petroleum system on the North West Shelf: Evidence from the Browse Basin. In: Purcell, P.G., Purcell, R.R. (Eds.), The Sedimentary Basins of Western Australia II. Petroleum Exploration Society of Australia, pp. 397–420.

Blevin, J.E., Boreham, C.J., Summons, R.E., Struckmeyer, H.I.M., Loutit, T.S., 2000. Hydrocarbon prospectivity of the Bight Basin - petroleum systems analysis in a frontier basin. In: Wood, G.R. (compiler), 2nd Sprigg Symposium - Frontier Basins, Frontier Ideas. Geological Society of Australia Abstracts 60, pp. 24–26.

Boreham, C., 2009. Organic geochemistry – source rock characterisation. In: Totterdell, J., Mitchell, C. (Eds.), Bight Basin geological sampling and seepage survey: RV Southern Surveyor SS01/2007. Geoscience Australia Record 2009/24, pp. 36-60. http://pid.geoscience.gov.au/dataset/ga/68689

Boreham, C.J., Krassay, A.A., Totterdell, J.M., 2001. Geochemical comparisons between asphaltites on the southern Australian margin and Cretaceous source rock analogues. In: Hill, K.C., Bernecker, T. (Eds.), Eastern Australasian Basins Symposium, A Refocused Energy Perspective for the Future. Petroleum Exploration Society of Australia Special Publication, pp. 531–541.

876 Boult, P.J., McKirdy, D., Blevin, J., Heggeland, R., Lang, S., Vinall, D., 2005. The oil-prone Morum Sub-
877 basin petroleum system, Otway Basin, South Australia. MESA J. 38, 28–33.

878 Bourdet, J., Kempton, R.H., Dvia, V., Pironon, J., Gong, S., Ross, A.S., 2019. Constraining the timing
879 and evolution of hydrocarbon migration in the Bight Basin. Mar. Pet. Geol. (submitted)

880 Brüning, M., Sahling, H., MacDonald, I.R., Ding, F., Bohrmann, G., 2010. Origin, distribution, and
881 alteration of asphalts at Chapopote Knoll, Southern Gulf of Mexico. Mar. Pet. Geol. 27, 1093–
882 1106. doi:10.1016/j.marpetgeo.2009.09.005

883 Bureau of Meteorology, 2016. Severe thunderstorm and tornado outbreak South Australia, 28
884 September 2016.

885 Burns, G., Adams, L., Buckley, G., 2017. Independent review of the extreme weather event South
886 Australia 28 September – 5 October 2016. Report presented to the Premier of South Australia.

887 Cassani, F., Gallango, O., Talukdar, S., Vallejos, C., Ehrmann, U., 1988. Methylphenanthrene maturity
888 index of marine source rock extracts and crude oils from the Maracaibo Basin. Org. Geochem.
889 13, 73–80. doi:10.1016/0146-6380(88)90027-7

890 Corrick, A.J., Hall, P.A., McKirdy, D.M., Gong, S., Trefry, C., Dyt, C., Angelini, Z., Ross, A.S., Kempton,
891 R., Armand, S., White, C., 2016. A revised oil family classification scheme and geochemical
892 weathering proxies for South Australian coastal bitumen strandings. In: 19th Australian Organic
893 Geochemistry Conference, Program and Abstracts. Fremantle, pp. 30–31.

894 Corrick, A.J., Selby, D., McKirdy, D.M., Hall, P.A., Gong, S., Trefry, C., Ross, A.S., 2019. Remotely
895 constraining the temporal evolution of offshore oil systems. Sci. Rep. 9, 1327.
896 doi:10.1038/s41598-018-37884-x

897 Currie, T.J., Alexander, R., Kagi, R.I., 1992. Coastal bitumens from Western Australia - long distance
898 transport by ocean currents. Org. Geochem. 18, 595–601.

899 Dahl, B., Speers, G.C., 1986. Geochemical characterization of a tar mat in the Oseberg field
900 Norwegian sector, North Sea. Org. Geochem. 10, 547–558. doi:10.1016/0146-6380(86)90053-7

901 Dowling, L.M., Boreham, C.J., Hope, J.M., Murray, A.P., Summons, R.E., 1995. Carbon isotopic
902 composition of hydrocarbons in ocean-transported bitumens from the coastline of Australia.
903 Org. Geochem. 23, 729–737. doi:10.1016/0146-6380(95)00061-I

904 Du Vivier, A.D.C., Selby, D., Sageman, B.B., Jarvis, I., Gröcke, D.R., Voigt, S., 2014. Marine $^{187}Os/^{188}Os$
905 isotope stratigraphy reveals the interaction of volcanism and ocean circulation during Oceanic
906 Anoxic Event 2. Earth Planet. Sci. Lett. 389, 23–33. doi:10.1016/j.epsl.2013.12.024

907 Edwards, D., McKirdy, D.M., Summons, R.E., 1998. Enigmatic asphaltites from the southern
908 Australian margin: molecular and carbon isotopic composition. PESA J. 26, 397–420.

909 Edwards, D.S., Vinall, D.R., Corrick, A.J., McKirdy, D.M., 2016. Natural bitumen stranding on the
910 ocean beaches of Southern Australia: a historical and geospatial review. Trans. R. Soc. South
911 Aust. 140, 152–185. doi:10.1080/03721426.2016.1203532

912 Edwards, D.S., McKirdy, D.M., Rowland, S.J., Heath, D.J., Gray, P.S., 2018. Waxy bitumen stranding in
913 southern Australia: A geochemical study of multiple oil families and their likely origins. Org.
914 Geochem. 118, 132–151. doi:10.1016/j.orggeochem.2017.12.010

915 Eigenbrode, J.L., Freeman, K.H., Summons, R.E., 2008. Methylhopane biomarker hydrocarbons in
916 Hamersley Province sediments provide evidence for Neoarchean aerobiosis. Earth Planet. Sci.
917 Lett. 273, 323–331. doi:10.1016/J.EPSL.2008.06.037

Farrimond, P., Bevan, J.C., Bishop, A.N., 1999. Tricyclic terpane maturity parameters: response to heating by an igneous intrusion. Org. Geochem. 30, 1011–1019. doi:10.1016/S0146-6380(99)00091-1

Finlay, A.J., Selby, D., Osborne, M.J., 2011. Re-Os geochronology and fingerprinting of United Kingdom Atlantic margin oil: Temporal implications for regional petroleum systems. Geology 39, 475–478. doi:10.1130/G31781.1

Fraser, A.R., Tilbury, L.A., 1979. Structure and stratigraphy of the Ceduna Terrace region, Great Australian Bight Basin. Aust. Pet. Explor. Assoc. J. 19(1), 53–65. doi:10.1071/AJ78007

Georgiev, S. V., Stein, H.J., Hannah, J.L., Galimberti, R., Nali, M., Yang, G., Zimmerman, A., 2016. Re-Os dating of maltenes and asphaltenes within single samples of crude oil. Geochim. Cosmochim. Acta. doi:10.1016/j.gca.2016.01.016

Goldhaber, M.B., Orr, W.L., 1995. Kinetic controls on thermochemical sulfate reduction as a source of sedimentary H_2S. In: Vairavamurthy, M.A., Schoonen, M.A.A., Eglinton, T.I., Luther, G.W., Manowitz, B. (Eds.), Geochemical Transformations of Sedimentary Sulfur. American Chemical Society, pp. 412–425. doi:10.1021/bk-1995-0612.ch023

Gong, S., Kempton, R.H., Ross, A.S., Bourdet, J., 2019. Characterisation of migrated hydrocarbons reveal insights into the source rocks of the Bight Basin. Mar. Pet. Geol. (submitted)

Haldorsen, H.H., Mayson, H.J., Howarth, S.M., 1985. The heavy oil/tar mat in the Prudhoe Bay Field, Alaska - characterization and impacts on reservoir performance. In: 3rd International UNITAR/UNDP Heavy Crude and Tar Sands Conference, Preprints, Vol. 2. Information Centre New York, pp. 481–503.

Hall, P.A., McKirdy, D.M., Grice, K., Edwards, D.S., 2014. Australasian asphaltite strandings: Their origin reviewed in light of the effects of weathering and biodegradation on their biomarker and isotopic profiles. Mar. Pet. Geol. 57, 572–593. doi:10.1016/j.marpetgeo.2014.06.013

Hao, F., Guo, T., Zhu, Y., Cai, X., Zou, H., Li, P., 2008. Evidence for multiple stages of oil cracking and thermochemical sulfate reduction in the Puguang gas field, Sichuan Basin, China. Am. Assoc. Pet. Geol. Bull. 92, 611–637. doi:10.1306/01210807090

Harrison, A.G., Thode, H.G., 1958. Mechanism of the bacterial reduction of sulphate from isotope fractionation studies. Trans. Faraday Soc. 54, 84–92.

Hayes, J.M., Freeman, K.H., Popp, B.N., Hoham, C.H., 1990. Compound-specific isotopic analyses: A novel tool for reconstruction of ancient biogeochemical processes. Org. Geochem. 16, 1115–1128. doi:10.1016/0146-6380(90)90147-R

Head, I.M., Jones, D.M., Röling, W.F.M., 2006. Marine microorganisms make a meal of oil. Nat. Rev. Microbiol. 4, 173–182. doi:10.1038/nrmicro1348

Holba, A.G., Tegelaar, E., Ellis, L., Singletary, M.S., Albrecht, P., 2000. Tetracyclic polyprenoids: Indicators of freshwater (lacustrine) algal input. Geology 28, 251–254. doi:10.1130/0091-7613(2000)28<251:TPIOFL>2.0.CO;2

Hurtig, N.C., Georgiev, S.V., Stein, H.J., Hannah, J.L., 2019. Re-Os systematics in petroleum during water-oil interaction: The effects of oil chemistry. Geochim. Cosmochim. Acta 247, 142–161. doi:10.1016/J.GCA.2018.12.021

Jones, G.E., Starkey, R.L., 1957. Fractionation of stable isotopes of sulfur by microorganisms and their role in deposition of native sulfur. Appl. Microbiol. 5, 111–118.

Kempton, R.H., Bourdet, J., Gong, S., Ross A.S., 2019. Revealing hidden oil migration in the frontier

961 Bight Basin, Australia. Mar. Pet. Geol. (submitted)

962 Krouse, H.R., Viau, C.A., Eliuk, L.S., Ueda, A., Halas, S., 1988. Chemical and isotopic evidence of
963 thermochemical sulphate reduction by light hydrocarbon gases in deep carbonate reservoirs.
964 Nature 333, 415–419. doi:10.1038/333415a0

965 Larter, S.R., Bjørlykke, K.O., Karlsen, D.A., Nedkvitne, T., Eglinton, T., Johansen, P.E., Leythaeuser, D.,
966 Mason, P.C., Mitchell, A.W., Newcombe, G.A., 1990. Determination of petroleum accumulation
967 histories: Examples from the Ula Field, Central Graben, Norwegian North Sea. In: Buller, A.T.,
968 Berg, E., Hjelmeland, O., Kleppe, J., Torsæter, O., Aasen, J.O. (Eds.), North Sea Oil and Gas
969 Reservoirs—II. Graham and Trotman, London, Dordrecht, pp. 319–330. doi:10.1007/978-94-
970 009-0791-1_27

971 Li, J., Xie, Z., Dai, J., Zhang, S., Zhu, G., Liu, Z., 2005. Geochemistry and origin of sour gas
972 accumulations in the northeastern Sichuan Basin, SW China. Org. Geochem. 36, 1703–1716.
973 doi:10.1016/J.ORGGEOCHEM.2005.08.006

974 Lillis, P.G., Selby, D., 2013. Evaluation of the rhenium–osmium geochronometer in the Phosphoria
975 petroleum system, Bighorn Basin of Wyoming and Montana, USA. Geochim. Cosmochim. Acta
976 118, 312–330. doi:10.1016/j.gca.2013.04.021

977 Liu, J., Selby, D., 2018. A matrix-matched reference material for validating petroleum Re-Os
978 measurements. Geostand. Geoanalytical Res. 42, 97–113. doi:10.1111/ggr.12193

979 Liu, Q., Zhu, D., Jin, Z., Liu, C., Zhang, D., He, Z., 2016. Coupled alteration of hydrothermal fluids and
980 thermal sulfate reduction (TSR) in ancient dolomite reservoirs – An example from Sinian
981 Dengying Formation in Sichuan Basin, southern China. Precamb. Res. 285, 39–57.
982 doi:10.1016/J.PRECAMRES.2016.09.006

983 Liu, J., Selby, D., Obermajer, M., Mort, A., 2018. Re-Os geochronology and oil-source correlation of
984 Duvernay Petroleum System, Western Canada Sedimentary Basin: Implications for the
985 application of the Re-Os geochronometer to petroleum systems. Am. Assoc. Pet. Geol. Bull.
986 102, 1627–1656. doi:10.1306/12081717105

987 Liu, J., Selby, D., Zhou, H., Pujol, M., 2019. Further evaluation of the Re-Os systematics of crude oil:
988 Implications for Re-Os geochronology of petroleum systems. Chem. Geol. 513, 1–22.
989 doi:10.1016/J.CHEMGEO.2019.03.004

990 Logan, G.A., Jones, A.T., Kennard, J.M., Ryan, G.J., Rollet, N., 2010. Australian offshore natural
991 hydrocarbon seepage studies, a review and re-evaluation. Mar. Pet. Geol. 27, 26–45.
992 doi:10.1016/j.marpetgeo.2009.07.002

993 Lorenson, T.D., Hostettler, F.D., Rosenbauer, R.J., Peters, K.E., Dougherty, J.A., Kvenvolden, K.A.,
994 Gutmacher, C.E., Wong, F.L., Normark, W.R., 2009. Natural Offshore Oil Seepage and Related
995 Tarball Accumulation on the California Coastline; Santa Barbara Channel and the Southern
996 Santa Maria Basin; source identification and inventory. U.S. Geological Survey Open-File Report
997 2009-1225 and MMS report 2009-030.

998 Machel, H.G., 2001. Bacterial and thermochemical sulfate reduction in diagenetic settings — old and
999 new insights. Sediment. Geol. 140, 143–175. doi:10.1016/S0037-0738(00)00176-7

1000 Machel, H.G., Krouse, H.R., Sassen, R., 1995. Products and distinguishing criteria of bacterial and
1001 thermochemical sulfate reduction. Appl. Geochemistry 10, 373–389. doi:10.1016/0883-
1002 2927(95)00008-8

1003 Mahdaoui, F., Michels, R., Reisberg, L., Pujol, M., Poirier, Y., 2015. Behavior of Re and Os during
1004 contact between an aqueous solution and oil: Consequences for the application of the Re–Os

1005 geochronometer to petroleum. Geochim. Cosmochim. Acta 158, 1–21.
1006 doi:10.1016/j.gca.2015.02.009

1007 Manzano, B.K., Fowler, M.G., Machel, H.G., 1997. The influence of thermochemical sulphate
1008 reduction on hydrocarbon composition in Nisku reservoirs, Brazeau river area, Alberta, Canada.
1009 Org. Geochem. 27, 507–521. doi:10.1016/S0146-6380(97)00070-3

1010 McKirdy, D.M., 1984a. Coastal bitumens and potential source rocks, Duntroon Basin, South Australia
1011 (AMDEL Report F 5769/84 for Getty Oil Development Company Ltd., South Australian
1012 Department of Mines and Energy Open File Envelope No. 5876).

1013 McKirdy, D.M., 1984b. Coastal bitumens and potential source rocks in the western Otway Basin,
1014 South Australia and Victoria (AMDEL Report F 5840/84 for Australian Aquitaine Petroleum Pty
1015 Ltd. and Ultramar Australia Inc., South Australian Department of Mines and Energy Open File.

1016 McKirdy, D.M., Aldridge, A.K., Ypma, P.J.M., 1983. A geochemical comparison of some crude oils
1017 from pre-Ordovician carbonate rocks. In: Bjoröy, M., Albrecht, P., Cornford, C., de Groot, K.,
1018 Eglinton, G., Galimov, E., Leythaeuser, D., Pelet, R., Speers, G. (Eds.), Advances in Organic
1019 Geochemistry 1981. John Wiley & Sons Limited, Chichester, pp. 99–107.

1020 McKirdy, D.M., Cox, R.E., Volkman, J.K., Howell, V.J., 1986. Botryococcane in a new class of
1021 Australian non-marine crude oils. Nature 320, 57–59. doi:10.1038/320057a0

1022 McKirdy, D.M., Kantsler, A.J., Emmett, J.K., Aldridge, A.K., 1984. Hydrocarbon genesis and organic
1023 facies in Cambrian carbonates of the Eastern Officer Basin, South Australia. In: Palacas, J.G.
1024 (Ed.), Petroleum Geochemistry and Source Rock Potential of Carbonate Rocks. AAPG Studies in
1025 Geology 18, pp. 13–31. doi:https://doi.org/10.1306/St18443C2

1026 McKirdy, D., Summons, R., Padley, D., Serafini, K., Boreham, C., Struckmeyer, H., 1994. Molecular
1027 fossils in coastal bitumens from southern Australia: signatures of precursor biota and source
1028 rock environments. Org. Geochem. 21, 265–286.

1029 Milner, C.W.D., Rogers, M.A., Evans, C.R., 1977. Petroleum transformations in reservoirs. J.
1030 Geochem. Explor. 7, 101–153. doi:10.1016/0375-6742(77)90079-6

1031 Moldowan, J.M., Seifert, W.K., 1980. First discovery of botryococcane in petroleum. J. Chem. Soc.
1032 Chem. Commun. 19, 912–914.

1033 Moldowan, J.M., Fago, F.J., Lee, C.Y., Jacobson, S.R., Watt, D.S., Slougui, N.-E., Jeganathan, A., Young,
1034 D.C., 1990. Sedimentary 24-*n*-propylcholestanes, molecular fossils diagnostic of marine algae.
1035 Science 247, 309–312. doi:10.2307/2873627

1036 Murray, A.P., Summons, R.E., Boreham, C.J., Dowling, L.M., 1994. Biomarker and *n*-alkane isotope
1037 profiles for Tertiary oils: relationship to source rock depositional setting. Org. Geochem. 22,
1038 521–542. doi:10.1016/0146-6380(94)90124-4

1039 Orr, W.L., 1974. Changes in sulfur content and isotopic ratios of sulfur during petroleum maturation -
1040 study of Big Horn Basin Paleozoic oils. Am. Assoc. Pet. Geol. Bull. 58, 2295–2318.

1041 Orr, W.L., 1986. Kerogen/asphaltene/sulfur relationships in sulfur-rich Monterey oils. Org. Geochem.
1042 10, 499–516. doi:10.1016/0146-6380(86)90049-5

1043 Padley, D., 1995. Petroleum geochemistry of the Otway Basin and the significance of coastal
1044 bitumen strandings on adjacent southern Australian beaches (PhD thesis). University of
1045 Adelaide.

1046 Palmer, S.E., 1993. Effect of biodegradation and water washing on crude oil composition. In: Engel,
1047 M.H., Macko, S.A. (Eds.), Organic Geochemistry. Plenum Press, New York, pp. 511–533.

1048 doi:10.1007/978-1-4615-2890-6_23

1049 Paytan, A., Kastner, M., Campbell, D., Thiemens, M.H., 2004. Seawater sulfur isotope fluctuations in
1050 the Cretaceous. Science 304, 1663–1665. doi:10.1126/science.1095258

1051 Peters, K.E., Walters, C.C., Moldowan, J.M., 2005. The Biomarker Guide, Vol. 2: Biomarkers and
1052 Isotopes in Petroleum Exploration and Earth History, 2nd edition. Cambridge University Press.

1053 Powell, T.G., McKirdy, D.M., 1973. Relationship between ratio of pristane to phytane, crude oil
1054 composition and geological environment in Australia. Nat. Phys. Sci. 243, 37–39.

1055 Price, P.L., O'Sullivan, T., Alexander, R., 1987. The nature and occurrence of oil in Seram, Indonesia.
1056 in: Proceedings of the Indonesian Petroleum Association, 16th Annual Convention. Indonesian
1057 Petroleum Association, Jakarta, Indonesia, pp. 141–173.

1058 Radke, M., 1987. Organic geochemistry of aromatic hydrocarbons. In: Brooks, J., Welte, D.H. (Eds.),
1059 Advances in Petroleum Geochemistry, Vol. 2. Academic Press, London, pp. 141–207.

1060 Radke, M., Welte, D.H., 1983. The methylphenanthrene index (MPI). A maturity parameter based on
1061 aromatic hydrocarbons. In: Bjoröy, M., Albrecht, P., Cornford, C., de Groot, K., Eglinton, G.,
1062 Galimov, E., Leythaeuser, D., Pelet, R., Speers, G. (Eds.), Advances in Organic Geochemistry
1063 1981. John Wiley & Sons Limited, Chichester, pp. 504–512.

1064 Radke, M., Leythaeuser, D., Teichmüller, M., 1984. Relationship between rank and composition of
1065 aromatic hydrocarbons for coals of different origins. Org. Geochem. 6, 423–430.
1066 doi:10.1016/0146-6380(84)90065-2

1067 Rooney, M.A., 1995. Carbon isotopic data of light hydrocarbons as indicators of thermochemical
1068 sulfate reduction. In: Grimalt, J.O., Dorronsoro, C. (Eds.), Organic Geochemistry: Development
1069 and Applications to Energy, Climate, Environment and Human History 1995. A.I.G.O.A.
1070 Donostia-San Sebastian, pp. 523-525

1071 Ross, A., Corrick, A., Trefry, C., Gong, S., McKirdy, D., Hall, T., Dyt, C., Angelini, Z., Kempton, R.,
1072 Pickard, A., White, C., Maslin, S., Griffin, D., Middleton, J., Luick, J., Armand, S., Vergara, T.,
1073 Schinteie, R., 2017. Asphaltite and tarball surveys. Final Report GABRP Project 5.2. Research
1074 Report Series Number 25a.

1075 Rullkötter, J., Spiro, B., Nissenbaum, A., 1985. Biological marker characteristics of oils and asphalts
1076 from carbonate source rocks in a rapidly subsiding graben, Dead Sea, Israel. Geochim.
1077 Cosmochim. Acta 49, 1357–1370. doi:10.1016/0016-7037(85)90286-8

1078 Scarlett, A.G., Holman, A.I., Georgiev, S. V., Stein, H.J., Summons, R.E., Grice, K., 2019. Multi-
1079 spectroscopic and elemental characterization of southern Australian asphaltites. Org.
1080 Geochem. doi:10.1016/J.ORGGEOCHEM.2019.04.006

1081 Schofield, A., Totterdell, J.M., 2008. Distribution, Timing and Origin of Magmatism in the Bight and
1082 Eucla Basins. Geoscience Australia Record 2008/24.

1083 Seifert, W.K., Moldowan, J.M., 1978. Applications of steranes, terpanes and monoaromatics to the
1084 maturation, migration and source of crude oils. Geochim. Cosmochim. Acta 42, 77–95.
1085 doi:10.1016/0016-7037(78)90219-3

1086 Selby, D., Creaser, R.A., 2005. Direct radiometric dating of hydrocarbon deposits using rhenium-
1087 osmium isotopes. Science 308, 1293–1295. doi:10.1126/science.1111081

1088 Selby, D., Creaser, R., Dewing, K., Fowler, M., 2005. Evaluation of bitumen as a Re–Os
1089 geochronometer for hydrocarbon maturation and migration: A test case from the Polaris MVT
1090 deposit, Canada. Earth Planet. Sci. Lett. 235, 1–15. doi:10.1016/j.epsl.2005.02.018

1091 Selby, D., Creaser, R.A., Fowler, M.G., 2007. Re–Os elemental and isotopic systematics in crude oils.
1092 Geochim. Cosmochim. Acta 71, 378–386. doi:10.1016/j.gca.2006.09.005

1093 Sprigg, R.C., Woolley, J.B., 1963. Coastal bitumen in southern Australia with special reference to
1094 observations at Geltwood Beach, south-east South Australia. Trans. R. Soc. South Aust. 86, 67–
1095 103.

1096 Struckmeyer, H.I.M., Totterdell, J.M., Blevin, J.E., Logan, G.A., Boreham, C.J., Deighton, I., Krassay,
1097 A.A., Bradshaw, M.T., 2001. Character, maturity and distribution of potential Cretaceous oil
1098 source rocks in the Ceduna Sub-Basin, Bight Basin, Great Australian Bight. In: Hill, K.C.,
1099 Bernecker, T. (Eds.), Eastern Australian Basins Symposium: a refocused energy perspective for
1100 the future. Petroleum Exploration Society of Australia, Special Publication, pp. 543–552.

1101 Summons, R.E., Volkman, J.K., Boreham, C.J., 1987. Dinosterane and other steroidal hydrocarbons of
1102 dinoflagellate origin in sediments and petroleum. Geochim. Cosmochim. Acta 51, 3075–3082.
1103 doi:10.1016/0016-7037(87)90381-4

1104 Summons, R.E., Bradshaw, J., Brooks, D.M., Goody, A.K., Murray, A.P., Foster, C.B., 1993.
1105 Hydrocarbon composition and origins of coastal bitumens from the Northern Territory,
1106 Australia. PESA J. 21, 31–42.

1107 Summons, R.E., Jahnke, L.L., Hope, J.M., Logan, G.A., 1999. 2-Methylhopanoids as biomarkers for
1108 cyanobacterial oxygenic photosynthesis. Nature 400, 554–557. doi:10.1038/23005

1109 Summons, R.E., Logan, G.A., Edwards, D.S., Boreham, C.J., Bradshaw, M.T., Blevin, J.E., Totterdell,
1110 J.M., Zumberge, J.E., 2001. Geochemical analogs for Australian coastal asphaltites - search for
1111 the source rock. In: Abstracts, AAPG Annual Convention, Denver, Colorado. Am. Assoc. Pet.
1112 Geol. Bull. 85 (Suppl.).

1113 Thode, H.G., Harrison, A.G., Monster, J., 1960. Sulphur isotope fractionation in early diagenesis of
1114 Recent sediments of Northeast Venezuela. Am. Assoc. Pet. Geol. Bull. 44, 1809–1817.

1115 Thode, H.., Monster, J., Dunford, H., 1961. Sulphur isotope geochemistry. Geochim. Cosmochim.
1116 Acta 25, 159–174. doi:10.1016/0016-7037(61)90074-6

1117 Thode, H.G., Monster, J., 1965. Sulfur-isotope geochemistry of petroleum, evaporites, and ancient
1118 seas. In: Young, A., Galley, J.E. (Eds.), Fluids in Subsurface Environments. Am. Assoc. Pet. Geol.
1119 Mem. 4, pp. 367–3677. doi:https://doi.org/10.1306/M4360

1120 Thode, H.G., Monster, J., 1970. Sulfur isotope abundances and genetic relations of oil accumulations
1121 in Middle East Basin. Am. Assoc. Pet. Geol. Bull. 54, 627–637.

1122 Tissot, B.P., Welte, D.H., 1984. Petroleum Formation and Occurrence, 2nd ed., Springer-Verlag,
1123 Berlin.

1124 Tolmer, A., 1882. Reminiscences of an Adventurous and Chequered Career at Home and in the
1125 Antipodes. Sampson Low, Marston, Searle & Rivington, London.

1126 Totterdell, J.M., Blevin, J.E., Struckmeyer, H.I.M., Bradshaw, B.E., Colwell, J.B., Kennard, J.M., 2000. A
1127 new sequence framework for the Great Australian Bight: Starting with a clean slate. Aust. Pet.
1128 Prod. Explor. J. 40, 95–118. doi:10.1071/AJ99007

1129 Totterdell, J.M., Bradshaw, B.E., 2004. The structural framework and tectonic evolution of the Bight
1130 Basin. In: Boult, P.J., Johns, D.R., Lang, S.C. (Eds.), Eastern Australasian Basins Symposium II.
1131 Petroleum Exploration Society of Australia Special Publication, pp. 41–61.

1132 Totterdell, J.M., Struckmeyer, H.I.M., Boreham, C.J., Mitchell, C.H., Monteil, E., Bradshaw, B.E., 2008.
1133 Mid-Late Cretaceous organic-rich rocks from the eastern Bight Basin : implications for

prospectivity. In: Blevin, J.E., Bradshaw, B.E., Uruski, E. (Eds.), Eastern Australasian Basins Symposium III. Petroleum Exploration Society of Australia Special Publication. pp. 137–158.

Trewartha, J., 1850. South Australian Government Gazette, 25 April 282.

van Graas, G.W., 1990. Biomarker maturity parameters for high maturities: Calibration of the working range up to the oil/condensate threshold. Org. Geochem. 16, 1025–1032. doi:10.1016/0146-6380(90)90139-Q

Volkman, J.K., O'Leary, T., Summons, R.E., Bendall, M.R., 1992. Biomarker composition of some asphaltic coastal bitumens from Tasmania, Australia. Org. Geochem. 18, 669–682. doi:10.1016/0146-6380(92)90092-C

Warnock, A.M., Hagen, S.C., Passeri, D.L., 2015. Marine Tar Residues: a Review. Water, Air, Soil Pollut. 226, 24. doi:10.1007/s11270-015-2298-5

Wei, Z., Walters, C.C., Moldowan, M.J., Mankiewicz, P.J., Pottorf, R.J., Xiao, Y., Maze, W., Nguyen, P.T.H., Madincea, M.E., Phan, N.T., Peters, K.E., 2012. Thiadiamondoids as proxies for the extent of thermochemical sulfate reduction. Org. Geochem. 44, 53–70. doi:10.1016/J.ORGGEOCHEM.2011.11.008

Wilhelms, A., Larter, S.R., 1994a. Origin of tar mats in petroleum reservoirs. Part I: introduction and case studies. Mar. Pet. Geol. 11, 418–441. doi:10.1016/0264-8172(94)90077-9

Wilhelms, A., Larter, S.R., 1994b. Origin of tar mats in petroleum reservoirs. Part II: Formation mechanisms for tar mats. Mar. Pet. Geol. 11, 442–456. doi:10.1016/0264-8172(94)90078-7

Worden, R.H., Smalley, P.C., 2001. H_2S in North Sea oil fields: importance of thermochemical sulphate reduction in clastic reservoirs. In: Cidu, R. (Ed.), Water-Rock Interaction: Proceedings of the tenth international symposium on water-rock interaction, WRI-10, Villasimius, Italy, 10-15 July 2001. Swets & Zeitlinger, Lisse. pp. 659–662.